IN THE UNITED STATES PATENT AND TRADEMARK OFFICE

Serial No. 10/677,734 Customer No. 23379

Applicant: Gardner et al. Confirmation No. 4912

Filed: Oct 01, 2003 Group Art Unit: 1656

Docket No. UTSD:1510-1 Examiner: Swope, Sheridan

Title: *Foreign PAS Ligands Regulate PAS Domain Function*

DECLARATION UNDER 37CFR1.132

I, Professor Stephen R. Sprang, declare and state as follows:

1. I am a Professor in the Department of Biochemistry at the University of Texas Southwestern Medical School. The Board of Regents of the University of Texas System is the assignee of this patent application. I have authored numerous scientific papers in the field of protein regulation, and I am familiar with this patent application. A copy of my curriculum vitae is attached.

2. HIF2α PAS B domain is an art-recognized, defined protein domain, and one skilled in the art does not require undue effort or experimentation to recognize and procure an HIF2α PAS B domain for use in the claimed methods, as documented for example by Erbel *et al.*, *Proc. Natl. Acad. Sci.* **100**(2003): 15504-9. In my opinion the Specification enables one skilled in the art to practice the invention without undue experimentation.

3. HIF2α PAS B domain is an art-recognized, defined protein domain, and one skilled in the art has no trouble recognizing an HIF2α PAS B domain for use in the claimed methods. There are many scientific publications describing the HIF2α PAS B domain, and how to use it (e.g. Erbel *et al.*, 2003, supra). In my opinion the specification amply describes and exemplifies the claimed methods to one skilled in the art.

4. Vogtherr (2003) generally describes the use of NMR-based screening for lead discovery; Amezcua (2002) describes the used of NMR to detect ligand binding to PAS kinase; Ema (1997) reports that *HIF1a* heterodimerizes with ARNT (note that HIF1α is structurally and functionally distinct from the recited HIF2α; Sowter *et al.*, *Cancer Res.* **63**(2003): 6130-4 and Raval *et al.*, *Mol Cell Biol* **25**(2005): 5675-86); and Fukunaga (1995) reports identification of functional domains of the aryl hydrocarbon receptor.

Prior to the present disclosure, HIF was known to be regulated in several ways by oxygen availability, but only via mechanisms that are based on oxygen-sensitive enzymes that covalently modify portions of the HIFα subunit at sites distant to the PAS domains (Bruick & McKnight,

Science **294**(2001): 1337-40; Jaakkola et al, *Science* **292**(2001): 468-72; Ivan *et al.*, *Science* **292**(2001): 464-8; Lando *et al.*, *Science* **295**(2002): 858-61). These findings demonstrated two independent modes of oxygen regulation that do not involve the PAS domains, which taught away from any expectation that the HIF PAS domains would be sensory.

In addition, HIF2α PASB presents a well-folded domain, which significantly contrasts with the dynamic regions of PASK PAS A (Amezcua *et al.*, *Structure* **10**(2002): 1349-61; Erbel *et al.*, 2003, supra), further removing any expectation of core ligand binding. Indeed, the structure of the ligand-free [apo] form of HIF2α PASB is in contrast with the apo-structures of the many small ligand-binding protein domains, which either exhibit pre-formed cavities or pockets for ligands to bind or alternatively adopt an unfolded (and often, chaperone-bound) conformation. The HIF2α PAS B structure shows neither of these.

Based on what was known prior to this disclosure, it is my opinion that one skilled in the art at the time of the filing date would not have expected HIF2α PAS to provide a core for sensory ligand binding.

I hereby declare that all statements made herein of my own knowledge are true and that all statements made on information and belief are believed to be true; and further that these statements are made with the knowledge that willful false statements and the like so made are punishable by fine or imprisonment, or both, under Section 1001 of Title 18 of the United States Code and that such willful, false statements may jeopardize the validity of the application and any patent issuing therefrom.

Date: June 19 2006

Professor Stephen R. Sprang

[CANCER RESEARCH 63, 6130–6134, October 1, 2003]

Advances in Brief

Predominant Role of Hypoxia-Inducible Transcription Factor (Hif)-1α *versus* Hif-2α in Regulation of the Transcriptional Response to Hypoxia[1]

Heidi M. Sowter, Raju Raval, John Moore, Peter J. Ratcliffe, and Adrian L. Harris[2]

Cancer Research UK, Weatherall Institute of Molecular Medicine, John Radcliffe Hospital, Oxford OX3 9DU [H. M. S., J. M., A. L. H.], and Wellcome Trust Centre for Human Genetics, Oxford OX3 7BN [R. R., P. J. R.], United Kingdom

Abstract

Tumor hypoxia induces the up-regulation of a gene program associated with angiogenesis, glycolysis, adaptation to pH, and apoptosis via the hypoxia-inducible transcription factors (Hifs) 1 and 2. Disruption of this pathway has been proposed as a cancer therapy. Here, we use short interfering RNAs to compare specific inactivation of Hif-1α or Hif-2α and show markedly different cell type-specific effects on gene expression and cell migration. Remarkably, among a panel of hypoxia-inducible genes, responses were critically dependent on Hif-1 α but not Hif-2 α in both endothelial and breast cancer cells but critically dependent on Hif-2 α in renal carcinoma cells.

Introduction

Hypoxia is an important process in the progression and treatment resistance of many human cancers (1). The majority of human cells share a common mechanism of oxygen sensing mediated by Hifs[3] 1 and 2. These proteins are heterodimers consisting of α subunits, Hif-1α and Hif-2α (also known as endothelial PER-ARNT-SIM domain protein 1) that dimerize with the constitutively expressed aryl hydrocarbon receptor nuclear translocator (also known as Hif-1β; reviewed in Ref. 2). Both Hif-α molecules are subject to similar regulatory processes involving enzymatic hydroxylation of conserved prolyl and asparaginyl residues that target them for degradation via the VHL ubiquitin E3 ligase complex (reviewed in Ref. 3). Moreover, in transfection assays, both transcription factors activate a range of hypoxia response elements with similar efficacy (4, 5).

Despite these striking similarities, genetic studies have provided firm evidence for nonredundant functions. Targeted inactivation of Hif-1α and Hif-2α in embryonic stem cells is associated with different patterns of response to hypoxia and low glucose stress (6), and different developmental defects are observed in Hif-1α$^{-/-}$ and Hif-2α$^{-/-}$ mouse embryos (for review see Ref. 3). In part, differences may relate to distinct patterns of cellular expression. For instance, in the kidney, whereas both transcription factors are abundantly expressed, Hif-1α is the predominant form in epithelial cells, whereas Hif-2α is predominant in interstitial fibroblast and endothelial cells (7). However, many cancers and cell lines express both isoforms. The expression of the two Hif-α isoforms at similar levels in this setting might be predicted to lead to a level of redundancy. Nevertheless, overexpression of Hif-2α, but not Hif-1α, promoted growth of renal cell carcinoma cells (8, 9) yet inhibited growth of breast cells (10), suggesting distinct effects on biology. These findings raise important questions as to what extent Hif-1α and Hif-2α have overlapping or redundant transcriptional functions in the cancer setting, whether expression of particular Hif transcriptional targets are always linked to expression of a particular Hif-α isoforms, or whether transcriptional selectivity varies according to cell background.

We have used siRNAs to specifically inhibit Hif-1α and Hif-2α production in human breast and renal carcinoma cell lines and in a human endothelial cell line, which express differing levels of Hif-1α and Hif-2α, ranging from isolated expression of Hif-1α to isolated expression of Hif-2α. The role of each molecule on induction of specific transcriptional targets with a variety of functions in the hypoxic response was then investigated.

Materials and Methods

siRNA Duplexes. The siRNA oligonucleotides were designed after the recommendations of Elbashir *et al.* (11) and were synthesized and high-performance liquid chromatography purified at Transgenomic Laboratories (Glasgow, United Kingdom). The Hif-1α siRNA duplex targeted nucleotides 1521–1541 of the Hif-1α mRNA sequence (NM001530) and comprised of: sense 5′-CUGAUGACCAGCAACUUGAdTdT-3′ and antisense 5′-UCAAGUUGCUGGUCAUCAGdTdT-3′. The Hif-2α siRNA duplex targeted nucleotides 1260–1280 of the Hif-2α mRNA sequence (NM001430) and comprised of sense 5′-CAGCAUCUUUGAUAGCAGUdTdT-3′ and antisense 5′-ACUGCUAUCAAAGAUGCUGdTdT-3′. The inverted Hif-1α control duplex did not target any gene and comprised of sense 5′-AGUUCAACGACCAGUAGUCdTdT-3′ and antisense 5′-GACUACUGGUCGUUGAdTdT-3′. Duplexes were prepared by mixing 50-μM concentrations of antisense and sense oligonucleotides with annealing buffer [30 mM HEPES (pH 7.0), 100 mM potassium acetate, and 2 mM magnesium acetate], heat denaturing for 1 min at 85°C, and annealing at 37°C for 1 h. Duplex formation was confirmed by electrophoresis through 5% low melting temperature agarose (NuSieve GTG; FMC Bioproducts, Rockland, ME). Additional siRNA duplexes used for confirmation of the specificity of particular effects were prepared as above and targeted to nucleotides 1510–1530 (AACGACACAGAAACTGATGAC) of the Hif-1α mRNA sequence and nucleotides 328–348 (AAATCAGCTTCCTGCGAACAC) of the Hif-2α mRNA sequence.

Cell Culture. MDA 435 cells, MDA 468 cells (breast cancer), 786-0 cells (renal cancer), and HUVECs (endothelial) were obtained from the Cancer Research United Kingdom cell service. Breast and renal cancer cells were grown in DMEM supplemented with 10% FCS (Globepharm), L-glutamine (2 μM), penicillin (50 IU/ml), and streptomycin sulfate (50 μg/ml). HUVECs were grown in the media supplemented as above but with 20% FCS plus endothelial cell growth supplement and heparin (Sigma) and grown on plates coated with 2% gelatin/PBS. Experiments were performed on dishes of cells in normoxia (humidified air with 5% CO_2) or hypoxia [hypoxic conditions were generated in a Napco 7001 incubator (Precision Scientific) with 0.1% O_2, 5% CO_2, and balance N_2].

siRNA Treatment of Cells. Cells were plated onto 10-cm^2 cell culture dishes and grown to 30–50% confluence before transfection. The duplexes were diluted to give a final concentration of 20 nM in Opti-Mem I (Invitrogen life Technologies, San Diego, CA). Twenty-five μl of Oligofectamine transfection reagent (Invitrogen Life Technologies) were added, and the mixture

Received 7/7/03; revised 8/12/03; accepted 8/15/03.

The costs of publication of this article were defrayed in part by the payment of page charges. This article must therefore be hereby marked *advertisement* in accordance with 18 U.S.C. Section 1734 solely to indicate this fact.

[1] H. M. S., J. M. and A. L. H. were funded by Cancer Research United Kingdom and P. J. R. by the Wellcome Trust. R. R. is a Rhodes scholar.

[2] To whom requests for reprints should be addressed, at Weatherall Institute of Molecular Medicine, John Radcliffe Hospital, Oxford OX3 9DU, United Kingdom. Phone: 44-1865-222457; Fax: 44-1865-222431; E-mail: harrisa@cancer.org.uk.

[3] The abbreviations used are: Hif, hypoxia-inducible factor; CA9, carbonic anhydrase 9; Glut-1, glucose transporter-1; HUVEC, human umbilical vein endothelial cell; siRNA, short interfering RNA; uPAR, urokinase-type plasminogen activator receptor; VEGF, vascular endothelial growth factor; VHL, von Hippel-Lindau.

incubated at room temperature for 25 min. The cells were rinsed with Opti-Mem I to remove any residual serum and incubated with the oligonucleotide duplexes in serum-free conditions for 4 h at 37°C. Serum was then added back to the culture, and cells were incubated for an additional 24 h before beginning an experiment.

RNA Preparation and RNase Protection Assay. Cells were rinsed with PBS and drained thoroughly. RNA was extracted from the cells using the solution D method described by Chomczynski and Sacchi (12) and assessed by absorbance at 260/280 nm. The RNase protection assay protocol and generation of ^{32}P-labeled RNA probes to Hif-1α, Hif-2α, and U6 small nuclear RNA has been described previously (4). Protected fragments were resolved on an 8% polyacrylamide gel and analyzed on a PhosphorImager (Molecular Dynamics, Sunnyvale, CA).

Western Blotting. Cells were washed thoroughly with PBS before being homogenized in a lysis buffer containing 8 M urea, 10% SDS, 1 M DTT, and protease inhibitors. Samples were electrophoresed on a 10% SDS-PAGE gel and transferred onto a polyvinylidene difluoride membrane (Millipore, Bedfordshire, United Kingdom). Proteins were detected using monoclonal antibodies to Hif-1α (Signal Transduction Laboratories), Hif-2α (4), CA9 (13), GLUT-1 (Alpha Diagnostic, San Antonio, TX), glyceraldehyde-3-phosphate dehydrogenase (Abcam, Cambridge, United Kingdom), and BNip3 (14) at 1:1,000, 1:1,000, 1:500, 1:250, 1:2,000, and 1:20,000, respectively. As a loading control, a mouse monoclonal antibody to β-tubulin (Sigma) was used at 1:20,000. Overnight primary antibody incubation was followed by incubation with goat antimouse or rabbit horseradish peroxidase (Dako) and enhanced chemiluminescence developing reagents (Amersham). Blots were exposed to film for between 30 s and 2 min.

Measurement of VEGF and uPAR. Supernatant was harvested from treated cells and centrifuged to remove cell debris. Secreted VEGF and uPAR were measured in the supernatant using the respective Quantikine ELISA kit (R&D Systems, Abingdon, United Kingdom) as per the manufacturer's instructions. The amount of VEGF and uPAR in the supernatant was normalized to the final number of cells in the dish from which it was harvested.

Cell Migration Assay. Cells treated with siRNA as described above were incubated in 0.1% oxygen for 16 h, removed from the culture dish using 2 mM EDTA, and resuspended in 1% FCS media. A total of 200 μl of serum-free media containing 1.5×10^4 cells was placed into the top of migration chambers with 8-μm filters (24-well plate format; Falcon), which were standing in wells containing 700 μl of media containing 10% FCS. The cells were incubated at 37°C for 4 h, after which the chambers were removed from the wells and coded for analysis by a blinded observer. Cells that had migrated to the bottom of the filter were fixed with 2.5% glutaraldehyde for 15 min, rinsed thoroughly with PBS, and stained with 0.1% crystal violet for 2 min. The total number of cells on the bottom of each filter was counted under a microscope, and each experiment was performed in triplicate on at least three occasions.

Results

Specificity of siRNAs Targeted to Hif-1α and Hif-2α. We synthesized siRNA oligonucleotides that specifically target Hif-1α or Hif-2α mRNAs for degradation and transfected these into cells 24 h before hypoxic stimulation. RNA extracted from the treated cells was subjected to RNAse Protection Assay analysis for Hif-1α and Hif-2α. MDA 468 and HUVECs expressed transcripts encoding both Hif-1α and Hif-2α (Fig. 1), whereas the MDA 435 cells did not express Hif-2α mRNA (Fig. 1), and the 786-0 cells did not express Hif-1α mRNA (Fig. 1). Treatment of the cells with the siRNAs ablated the expression of Hif-1α and Hif-2α mRNA specifically in that the Hif-1α siRNA did not affect the Hif-2α gene expression and *vice versa* (Fig. 1). Inverted siRNA controls of the Hif-1α and Hif-2α siRNAs had no effect on the expression of either gene; the inverted Hif-1α siRNA was used as the control in all experiments described (Figs. 1–4). When cells were transfected with both siRNAs, expression of Hif-1α and Hif-2α was ablated. No cell toxicity was noted after transfection with either of the siRNAs or with Oligofectamine alone (described as the negative control). To confirm the specificity of the technique, siRNAs targeted to another region of the Hif-1α and

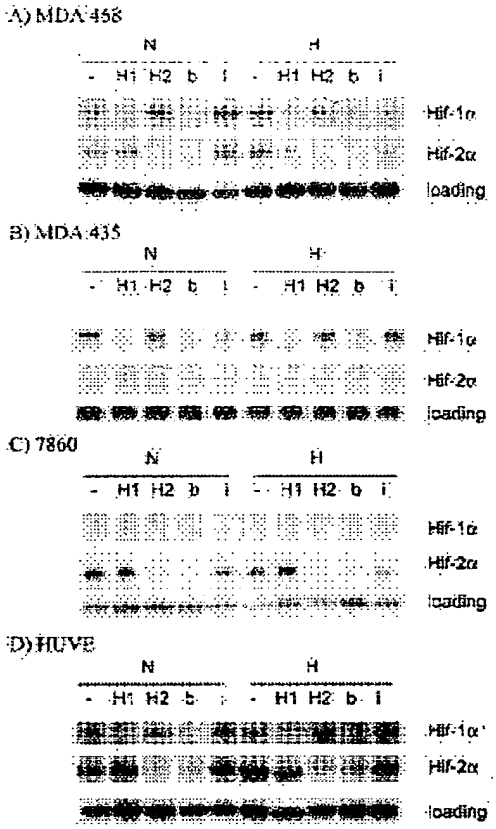

Fig. 1. RNase protection analysis of RNA extracted from MDA 468 cells (*A*), MDA 435 cells (*B*), 786-0 cells (*C*), and HUVECs (*D*). Cells were mock transfected (−) or subjected to siRNA directed to Hif-1α (1), Hif-2α (2), both Hif-1α and Hif-2α (b), or inverted control (*i*) before subsequent incubation for 16 h in 20% oxygen (N) or 0.1% oxygen (H). Specific down-regulation of Hif-1α or Hif-2α mRNA occurred after siRNA for each respective transcript or both transcripts. The inverted siRNA control had no effect on mRNA levels. Quantification of U6 small nuclear RNA was used as a loading control.

Hif-2α mRNAs were synthesized and transfected into MDA 468 cells, which were then subjected to hypoxic stimulation. The results obtained with these siRNAs were the same as described above in respect to specificity of Hif-1α and Hif-2α targeting (data not shown).

Expression of Hypoxically Induced Genes by Human Cell Lines After Treatment with siRNA for Hif-1α and Hif-2α. The HIF system up-regulates the production of proteins with a wide range of functions in the homeostatic and apoptotic response (2, 3, 13, 15) to hypoxia and cell death in many different human cell types. To investigate the importance of Hif-1α and Hif-2α in conferring such responses in different cell backgrounds, we analyzed the expression of CA9 (acid metabolism), BNip3 (cell death), GLUT-1 (glucose/energy metabolism), VEGF (angiogenesis), and uPAR (proteolytic pathway of invasion) in MDA 435 cells, MDA 468 cells (breast carcinoma), 786-0 cells (renal carcinoma), and HUVECs (endothelial) after treatment with Hif-1α and/or Hif-2α siRNA. Protein levels were measured using Western blot analysis (CA9, BNip3, and GLUT-1) or ELISA (VEGF and uPAR).

Analysis of the breast carcinoma cell lines revealed that MDA 468 cells expressed both Hif-1α and Hif-2α protein (Fig. 2), whereas MDA 435 cells expressed only Hif-1α protein (data not shown). In both cell lines, hypoxic induction of CA9, BNip3, GLUT-1, VEGF, and uPAR protein was inhibited by treatment with Hif-1α siRNA but not affected by Hif-2α siRNA. Silencing both Hif-1α and Hif-2α had the same effect as silencing with Hif-1α, and the inverted control

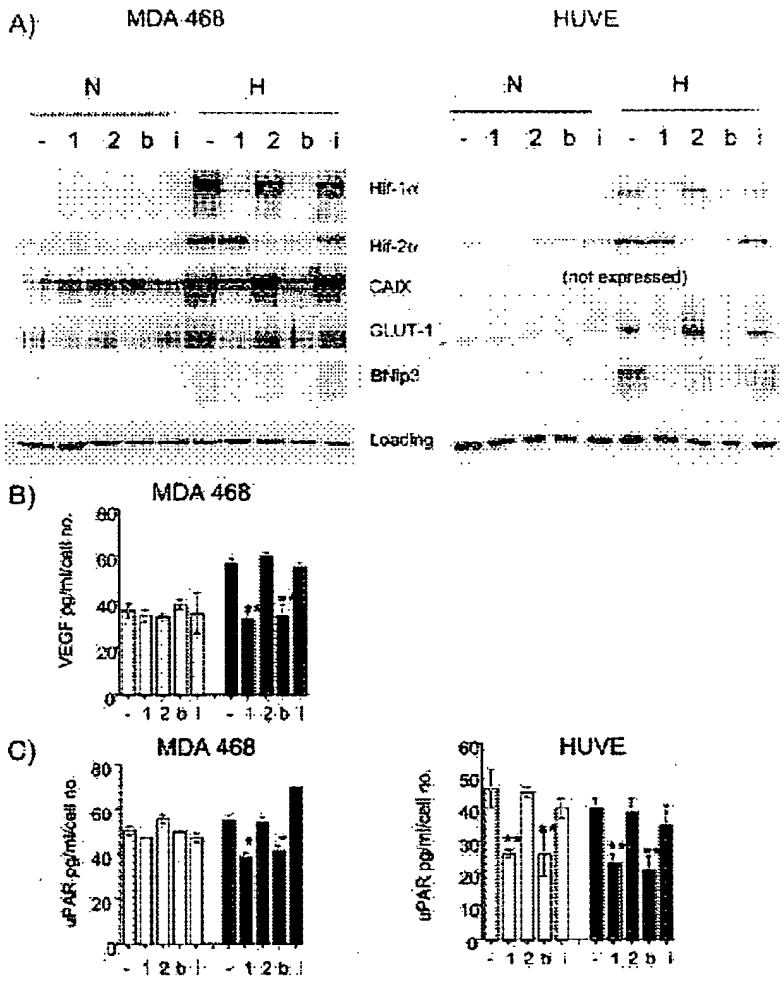

Fig. 2. *A*, Western blot analysis of protein extracted from MDA 468 cells and HUVECs after treatment as described in Fig. 1. Specific down-regulation of Hif-1α or Hif-2α protein occurred after siRNA for each respective transcript or both transcripts. The inverted siRNA control had no effect on protein levels. Hypoxic induction of CA9, GLUT-1, and BNip3 protein was blocked after siRNA for Hif-1α but not after siRNA for Hif-2α. siRNA against both genes also resulted in the down-regulation of the target genes. *B*, VEGF levels and uPAR levels (*C*) in media conditioned by MDA 468 (*B* and *C*) and HUVECs (*C*), normalized to final cell number. Normoxic or hypoxic treatment of cells is indicated by □ and ■, respectively. Experiments were performed in triplicate at least three times, and results from one representative experiment are shown. One-tailed, student *t* tests comparing each treatment with the hypoxic mock control were performed, and significance is indicated by * for $P < 0.05$ and ** for $P < 0.01$.

siRNA had no effect on the expression of any of the genes (Fig. 2; data not shown). The same results were obtained when MDA 468 cells were transfected with the confirmatory siRNAs (data not shown).

Similar to the MDA 468 cell lines, HUVECs expressed both Hif-1α and Hif-2α protein after hypoxic stimulus (Fig. 2). Hypoxia did not induce HUVECs to express CA9 or secrete VEGF but did increase the levels of expression of BNip3, GLUT-1, and uPAR. Pretreatment of HUVECs with siRNA to Hif-1α ablated the hypoxic induction of BNip3, GLUT-1, and uPAR, but Hif-2α siRNA treatment had no effect on protein production (Fig. 2).

The renal carcinoma cell line 786-0 expressed Hif-2α but not Hif-1α, and because this cell line lacks functional VHL, expression of Hif-2α was seen constitutively under normoxic conditions (Fig. 3). VEGF and GLUT-1 proteins were also constitutively expressed, but BNip3 and CA9 proteins were not expressed at detectable levels. uPAR was constitutively expressed by 786-0 cells but at 2-fold lower levels than by breast or endothelial cells. Treatment of cells with siRNA to Hif-2α reduced the expression of GLUT-1 and VEGF, whereas siRNA to Hif-1α had no effect (Fig. 3). Expression of uPAR was not affected by siRNA to Hif-1α or Hif-2α.

Cell Migration Induced by Hypoxia Is Affected by Pretreatment with siRNA to Hif-1α or Hif-2α Depending on the Cell Type. Intratumoral hypoxia is correlated with increased risk of invasion in human cancer (1), and hypoxia increases the invasion of colon carcinoma cells (16). To elucidate which hypoxia-induced transcription factor is involved in this process, we analyzed MDA 468 and HUVE cells treated with siRNA for Hif-1α or Hif-2α and normoxia or hypoxia in a cell migration assay. Cells subjected to hypoxia showed increased migration compared with the cells that had remained in normoxia, and treatment with inverted siRNA or mock transfection had no effect on the migration response. In MDA 435 cells, the hypoxic response was inhibited by treatment with siRNA directed to Hif-1α but not to Hif-2α. However, in MDA 468 and HUVECs, hypoxically induced migration was inhibited by pretreatment of the cells with either Hif-1α or Hif-2α siRNA. Treatment of cells with both siRNAs inhibited the hypoxically induced migration response in both cell lines but not more than with either alone (Fig. 4).

Discussion

In this study, we used siRNAs that specifically target degradation of mRNAs encoding Hif-1 α or Hif-2α. After treatment with siRNA, the expression of Hif-1α or Hif-2α mRNA and protein was greatly reduced under hypoxic conditions. The effects of these siRNAs were analyzed in two human breast carcinoma cell lines, a human endothelial cell line, and a human renal carcinoma cell line containing an inactivating mutation in VHL.

Our results indicate that in the breast carcinoma and endothelial cell

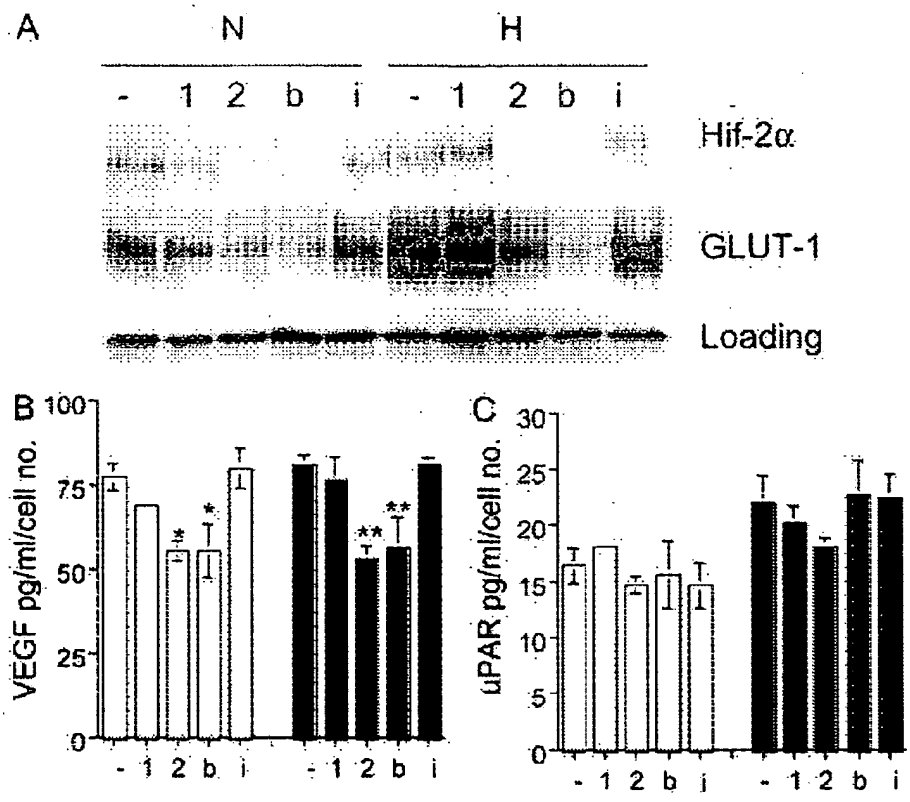

Fig. 3. *A*. Western blot analysis of protein extracted from 786-0 cells after treatment as described in Fig. 1. 786-0 cells do not express Hif-1α, but specific down-regulation of Hif-2α protein occurred after siRNA for Hif-2α. The inverted siRNA and Hif-1α siRNA had no effect on Hif-2α protein levels. GLUT-1 protein is reduced after siRNA for Hif-2α but not after siRNA for Hif-1α. Somewhat unusually, there was a modest induction of GLUT-1 after hypoxic stimulus, which was also inhibited by siRNA for Hif-2α. siRNA for both genes also resulted in the down-regulation of the target genes. *B*, VEGF levels and uPAR levels (*C*) in media conditioned by the above cells normalized to final cell number. Normoxic or hypoxic treatment of cells is indicated by □ and ■, respectively. Experiments were performed in triplicate at least three times, and results from one representative experiment are shown. One-tailed, student *t* tests comparing each treatment with the hypoxic mock control were performed, and significance is indicated by * for $P < 0.05$ and ** for $P < 0.01$.

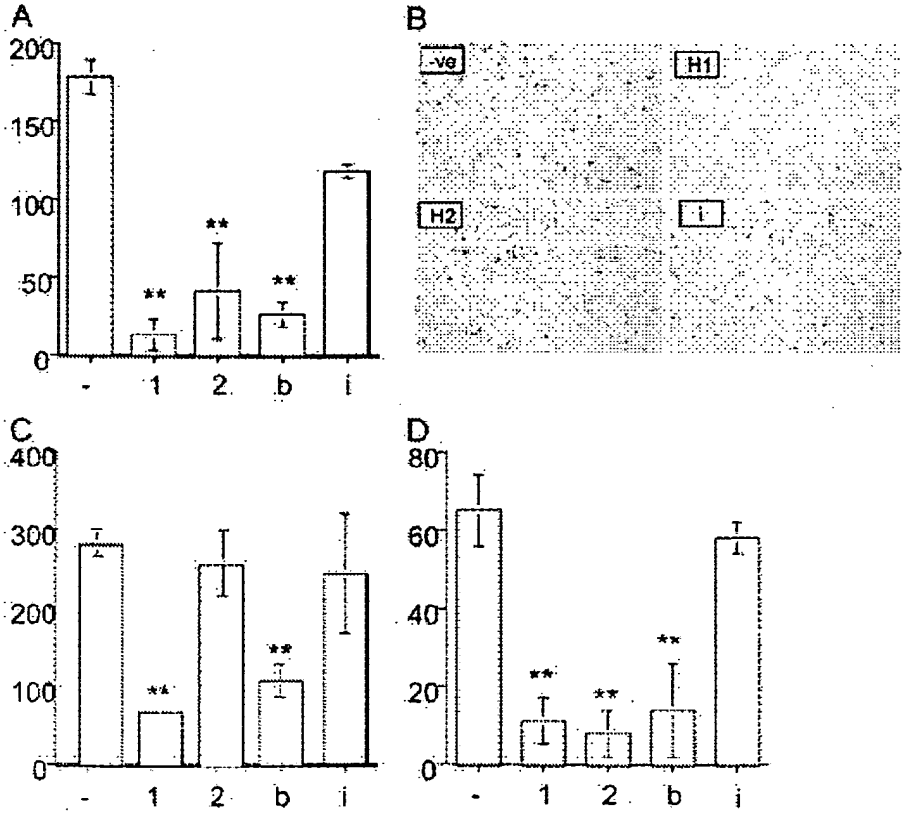

Fig. 4. Migration analysis of cells treated with a mock transfection (−) or siRNA for Hif-1α (1), Hif-2α (2), both Hif-1α and Hif-2α (b), or inverted control (i) before subsequent incubation for 16 h in 0.1% oxygen. The number of cells that had migrated through an 8-μm filter was counted, and the mean and SD of three replicates in a representative experiment is shown graphically. *A* and *B*, hypoxically induced migration of MDA 468 cells is inhibited by treatment with siRNA for both Hif-1α and Hif-2α. *B* shows photographs of the bottom of a representative selection of migration chambers, with blue cells visible around the smaller round pores of the filter. *C*, hypoxically induced migration of MDA 435 cells was inhibited by treatment with siRNA for Hif-1α, not Hif-2α, whereas migration of HUVECs was inhibited by siRNA for both Hif-1α and Hif-2α (*D*).

lines, the major Hif-α isoform required for induction of a set of well-characterized hypoxic genes is Hif-1α. Surprisingly, even in cells expressing both Hif-α isoforms, Hif-2α did not substitute in regulating any of these genes when Hif-1α was inactivated. Nevertheless, functional analysis of the endothelial and breast carcinoma cell lines revealed that both Hif-1α and Hif-2α are required for hypoxia-induced cell migration in cell lines that express both proteins, suggesting that there are other actions of Hif-2α that have not been revealed in our studies of gene expression. Overall, however, the importance of Hif-1α in these cells is in concordance with other studies that have reported Hif-1α as a positive factor in tumor growth (17) and carcinoma cell invasion (16) in different cells. The hypothesis that Hif-1α is the major hypoxia-induced transcription factor involved in breast carcinogenesis is supported by evidence that one of the breast carcinoma cell lines used in this study has lost Hif-2α expression, and stable transfection of this cell line with Hif-2α resulted in its impaired growth as xenograft tumors compared with the parental line (10).

In contrast with the above results, we found that in the VHL-defective 786-0 renal carcinoma line, in which the native Hif-1α gene is not expressed, some of the hypoxia-inducible transcripts were now critically dependent of Hif-2α. VHL is required for proteolytic regulation of both Hif-1α and Hif-2α, and in VHL defective cells both isoforms are stabilized. However, there is an unusual bias toward enhanced Hif-2α mRNA expression in clear cell renal carcinoma that is not observed in the renal tubular epithelium from which these tumors are derived (7) but arises during tumor development (18). This may be because of an additional action of VHL on the Hif system (19, 20) and/or additional non-VHL mediated actions on Hifα isoforms that arise during the oncogenic process. The current results suggest the existence of another distinct interface between the HIF system and renal carcinogenesis that makes connections between Hif-2α expression and certain hypoxia-inducible mRNAs. The finding that the Hif-2α pathway appears to be specifically activated in clear cell renal carcinogenesis by several steps strongly suggests a causal role for Hif-2α in development of the cancer. Interestingly, this is supported by comparison of results from two groups that have examined the expression of mutant forms of Hif-1α or Hif-2α that escape VHL-mediated destruction on the tumor suppressor effect of expressing wild-type VHL in renal cell carcinoma cells. These studies have shown that stabilized Hif-2α but not Hif-1α reverses VHL tumor suppressor function (8, 9).

In conclusion, these studies have, for the first time, directly compared functional inactivation of Hif-1α and Hif-2α in different cancer cell lines. The findings indicate that the actions are distinct and differ according to cell background and suggest that these differences are important in tumor development.

Acknowledgments

We thank Arnold Greenberg (deceased) of the cell death group at Manitoba Institute of Cell Biology, University of Manitoba (Winnipeg, Manitoba, Canada) for the kind gift of the BNip3 monoclonal antibody.

References

1. Hoeckel, M., and Vaupel, P. Biological consequences of tumor hypoxia. Semin. Oncol., *28:* 36–41, 2001.
2. Semenza, G. L. HIF-1 and tumor progression: pathophysiology and therapeutics. Trends Mol. Med., *8:* S62–S67, 2002.
3. Pugh, C. W., and Ratcliffe, P. J. Regulation of angiogenesis by hypoxia: role of the HIF system. Nat. Med., *9:* 677–684, 2003.
4. Wiesener, M. S., Turley, H., Allen, W. E., Willam, C., Eckhardt, K. U., Talks, K. L., Wood, S. M., Gatter, K. C., Harris, A. L., Pugh, C. W., Ratcliffe, P. J., and Maxwell, P. H. Induction of endothelial PAS domain protein-1 by hypoxia: characterization and comparison with hypoxia-inducible factor-1α. Blood, *92:* 2260–2268, 1998.
5. Ema, M., Hirota, K., Mimura, J., Abe, H., Yodoi, J., Sogawa, K., Poellinger, L., and Fujii-Kuriyama, Y. Molecular mechanisms of transcription activation by HLF and HIF1α in response to hypoxia: their stabilization and redox signal-induced interaction with CBP/p300. EMBO J., *18:* 1905–1914, 1999.
6. Brusselmans, K., Bono, F., Maxwell, P. H., Dor, Y., Dewerchin, M., Collen, D., Herbert, J-M., and Carmeliet, P. Hypoxia-inducible factor-2α is involved in the apoptotic response to hypoglycemia but not to hypoxia. J. Biol. Chem., *276:* 39192–39196, 2001.
7. Rosenberger, C., Mandriota, S., Jurgensen, J. S., Wiesner, M. S., Horstrup, J. H., Frei, U., Ratcliffe, P. J., Maxwell, P. H., Bachmann, S., and Eckardt, K. U. Expression of hypoxia-inducible factor-1α and -2α in hypoxic and ischemic rat kidneys. J. Am. Soc. Nephrol., *13:* 1974–1976, 2002.
8. Maranchie, J. K., Vasselli, J. R., Riss, J., Bonifacino, J. S., Linehan, W. M., and Klausner, R. D. The contribution of VHL substrate binding and HIF-1α to the phenotype of VHL loss in renal cell carcinoma. Cancer Cell, *1:* 247–255, 2002.
9. Kondo, K., Kim, J., Nakamura, E., Lechpammer, M., and Kaelin, W. G. Inhibition of HIF is necessary for tumor suppression by the von Hippel Lindau protein. Cancer Cell, *1:* 237–246, 2002.
10. Blancher, C., Moore, J. W., Talks, K. L., Houlbrook, S., and Harris, A. L. Relationship of hypoxia-inducible factor (HIF)-1α and HIF-2α expression to vascular endothelial growth factor induction and hypoxia survival in human breast cancer cell lines. Cancer Res., *60:* 7106–7113, 2000.
11. Elbashir, S. M., Harborth, J., Lendeckel, W., Yalcin, A., Weber, K., and Tuschl, T. Duplexes of 21-nucleotide RNAs mediate RNA interference in cultured mammalian cells. Nature (Lond.), *411:* 494–498, 2001.
12. Chomczynski, P., and Sacchi, N. Single step method of RNA isolation by acid guanidinium thiocyanate-phenol-chloroform extraction. Anal. Biochem., *162:* 156–159, 1987.
13. Wykoff, C. C., Beasley, N. J. P., Watson, P. H., Turner, K. J., Pastorek, J., Sibtain, A., Wilson, G. D., Turley, H., Talks, K., Maxwell, P. H., Pugh, C. W., Ratcliffe, P. J., and Harris, A. L. Hypoxia-inducible expression of tumor-associated carbonic anhydrases. Cancer Res., *60:* 7075–7083, 2000.
14. Ray, R., Chen, G., Vande Velde, C., Cizeau, J., Hoon Park, J. H., Reed, J. C., Gietz, R. D., and Greenberg, A. H. BNIP3 heterodimerizes with Bcl-2/Bcl-XL and induces cell death independent of a Bcl-2 homology 3 (BH3) domain at both mitochondrial and nonmitochondrial sites. J. Biol. Chem., *275:* 1439–1448, 2000.
15. Sowter, H. M., Ratcliffe, P. J., Watson, P., Greenberg, A. H., and Harris, A. L. HIF-1-dependent regulation of hypoxic induction of the cell death factors BNIP3 and NIX in human tumors. Cancer Res. *61:* 6669–6673, 2001.
16. Krishnamachary, B., Berg-Dixon, S., Kelly, B., Agani, F., Feldser, D., Ferreira, G., Iyer, N., LaRusch, J., Pak, B., Taghavi, P., and G. L. S. Regulation of colon carcinoma cell invasion by hypoxia-inducible factor 1. Cancer Res., *63:* 1138–1143, 2003.
17. Ryan, H. E., Poloni, M., McNulty, W., Elson, D., Gassmann, M., Arbeit, J. M., and Johnson, R. S. Hypoxia-inducible factor-1α is a positive factor in solid tumor growth. Cancer Res., *60:* 4010–4015, 2000.
18. Mandriota, S. J., Turner, K. J., Davies, D. R., Murray, P. G., Morgan, N. V., Sowter, H. M., Wykoff, C. C., Maher, E. R., Harris, A. L., Ratcliffe, P. J., and Maxwell, P. H. HIF inactivation identifies early lesions in VHL kidneys: evidence for site specific tumor suppressor function in the nephron. Cancer Cell, *1:* 459–468, 2002.
19. Kreig, M., Haas, R., Brauch, H., Acker, T., Flamme, I., and Plate, K. H. Up-regulation of hypoxia-inducible factors HIF-1α and HIF-2α under normoxic conditions in renal carcinoma cells by von Hippel-Lindau tumor suppressor gene loss function. Oncogene, *19:* 5435–5443, 2000.
20. Maxwell, P. H., Dachs, G., Gleadle, J. M., Nicholls, L. G., Harris, A. L., Stratford, I. J., Hankinson, O., Pugh, C. W., and Ratcliffe, P. J. Hypoxia-inducible factor-1 modulates gene expression in solid tumors and influences both angiogenesis and tumor growth. Proc. Natl. Acad. Sci. USA, *94:* 8104–8109, 1997.

Structural basis for PAS domain heterodimerization in the basic helix–loop–helix-PAS transcription factor hypoxia-inducible factor

Paul J. A. Erbel*†, Paul B. Card*†, Ozgur Karakuzu*, Richard K. Bruick*, and Kevin H. Gardner*†‡

Departments of *Biochemistry and †Pharmacology, University of Texas Southwestern Medical Center, 5323 Harry Hines Boulevard, Dallas, TX 75390

Edited by Susan S. Taylor, University of California at San Diego, La Jolla, CA, and approved October 9, 2003 (received for review June 10, 2003)

Biological responses to oxygen availability play important roles in development, physiological homeostasis, and many disease processes. In mammalian cells, this adaptation is mediated in part by a conserved pathway centered on the hypoxia-inducible factor (HIF). HIF is a heterodimeric protein complex composed of two members of the basic helix–loop–helix Per-ARNT-Sim (PAS) (ARNT, aryl hydrocarbon receptor nuclear translocator) domain family of transcriptional activators, HIFα and ARNT. Although this complex involves protein–protein interactions mediated by basic helix–loop–helix and PAS domains in both proteins, the role played by the PAS domains is poorly understood. To address this issue, we have studied the structure and interactions of the C-terminal PAS domain of human HIF-2α by NMR spectroscopy. We demonstrate that HIF-2α PAS-B binds the analogous ARNT domain *in vitro*, showing that residues involved in this interaction are located on the solvent-exposed side of the HIF-2α central β-sheet. Mutating residues at this surface not only disrupts the interaction between isolated PAS domains *in vitro* but also interferes with the ability of full-length HIF to respond to hypoxia in living cells. Extending our findings to other PAS domains, we find that this β-sheet interface is widely used for both intra- and intermolecular interactions, suggesting a basis of specificity and regulation of many types of PAS-containing signaling proteins.

Cellular responses to oxygen availability are essential for the development and homeostasis of mammalian cells, demonstrated most critically by the link between the cellular adaptation to reduced tissue oxygenation and disease progression (1, 2). In mammalian cells, these responses are mediated in part by the hypoxia-inducible factor (HIF), a heterodimeric transcription factor composed of HIFα and aryl hydrocarbon receptor nuclear translocator (ARNT, also known as HIFβ) (3). HIF activity is tightly controlled under normoxic conditions by multiple O_2-dependent hydroxylation events of the HIFα subunit, which coordinately promote the ubiquitin-mediated destruction of this protein (4) and impair its ability to interact with transcriptional coactivators (5, 6) (Fig. 1*a*). These controls are relieved during hypoxia, allowing HIF to activate the transcription of genes that facilitate metabolic adaptation to low oxygen levels and increase local oxygen supply by angiogenesis (7).

All three isoforms of HIFα [HIF-1α, -2α (EPAS1), and -3α] (8, 9) and ARNT belong to the basic helix–loop–helix (bHLH)–Per-ARNT-Sim (PAS) family of eukaryotic transcription factors, which contain bHLH and PAS domains (Fig. 1). The bHLH domains of these proteins serve as dimerization elements, helping determine the specificity of complex formation while providing a DNA-binding interface composed of the basic regions from each monomer (10). PAS domains are widespread components of signal transduction proteins, currently identified in >2,000 proteins from organisms in all three kingdoms of life. These domains, shown to be protein–protein interaction elements in several systems (11), also appear to contribute to the dimerization process and thus increase the specificity of bHLH-PAS transcription factor formation (12, 13). In the case of the HIFα/ARNT complex, coimmunoprecipitation and gel mobility-shift experiments using truncated forms of HIFα and ARNT suggest that although the bHLH domains alone are able to dimerize, the PAS domains are required to build a stable heterodimer capable of robust DNA binding (14, 15). These data suggest a model of the complex where the bHLH, PAS-A, and PAS-B domains of ARNT interact with their counterparts in HIFα (Fig. 1*a*). However, most of this model remains speculative in light of the sparse data describing how PAS domains bind to each other, or more generally, to any protein partner.

To provide insight into this general topic of PAS domain signaling, particularly its importance in the hypoxia response pathway, we have studied the structure and interactions of the C-terminal PAS domain of human HIF-2α (HIF-2α PAS-B) by NMR spectroscopy. We report that HIF-2α PAS-B adopts a structure similar to other members of this family, with a central β-sheet flanked on one face by several α-helices. We further show that HIF-2α PAS-B binds directly to the human ARNT PAS-B domain *in vitro*, identifying the interface as a group of residues located in the central strands of the β-sheet. With structure-based mutations of this interface in the PAS-B domains of HIF-1α and -2α, we demonstrate that such changes interfere with the binding of isolated PAS-B domains *in vitro* but more importantly disrupt the ability of full-length HIF proteins to respond to hypoxia in living cells. These observations led us to compare PAS domains from multiple systems, showing that the β-sheet interface participates in a wide range of inter- and intramolecular interactions and suggesting a way that specificity and regulation may be achieved among these versatile domains.

Materials and Methods

Protein Expression and Purification. DNA-encoding fragments of human HIF-2α PAS-B (residues 240–350) and ARNT PAS-B (residues 356–470) were subcloned into the pGβ1-parallel and pHis-parallel expression vectors, respectively (16, 17). *Escherichia coli* BL21(DE3) cells transformed with these plasmids were grown in M9 media containing 1 g/liter $^{15}NH_4Cl$ for U-^{15}N samples (supplemented with 3 g/liter $^{13}C_6$ glucose for U-^{15}N/^{13}C labeled samples). These cultures were grown at 37°C to an A_{600} of 0.6–1.0, then induced overnight at 20°C by the addition of 0.5 mM isopropyl β-D-thiogalactoside.

The purification of HIF-2α PAS-B has been detailed (18). NMR samples typically contained 0.9 mM protein in 50 mM Tris buffer (pH 7.3), 15 mM NaCl, 5 mM DTT, 5 mM NaN_3 and a protease inhibitor mixture (Sigma) in 90% H_2O/10% D_2O,

This paper was submitted directly (Track II) to the PNAS office.

Abbreviations: HIF, hypoxia-inducible factor; PAS, Per-ARNT-Sim; HIF-2α PAS-B, C-terminal PAS domain of human HIF-2α; ARNT, aryl hydrocarbon receptor nuclear translocator; bHLH, basic helix–loop–helix; HSQC, heteronuclear sequential quantum correlation; CHO, Chinese hamster ovary; HRE, hypoxia responsive element.

Data deposition: The atomic coordinates for the HIF-2α PAS-B domain have been deposited in the Protein Data Bank (PDB ID 1P97).

‡To whom correspondence should be addressed. E-mail: kevin.gardner@utsouthwestern.edu.

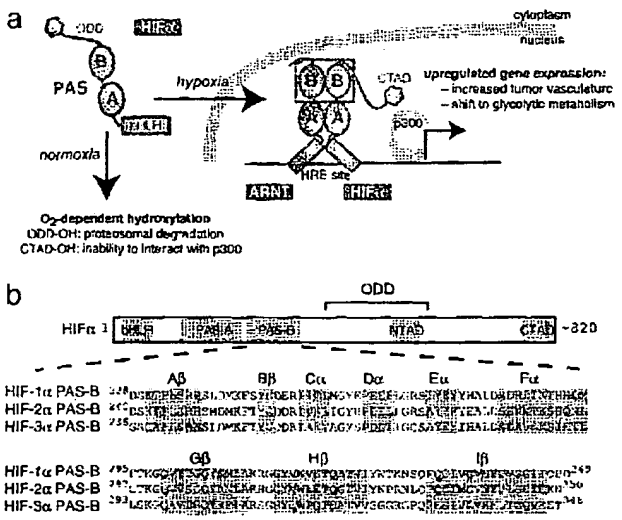

Fig. 1. Oxygen-dependent regulation and domain architecture of HIF proteins. (*a*) HIF regulation is tightly linked to intracellular oxygen levels. Under normoxic conditions, HIFα is posttranslationally hydroxylated, promoting its degradation [modification of the oxygen-dependent degradation domain (ODD)] and interfering with its ability to interact with CBP/p300 coactivators (modification of the transcriptional activation domains NTAD and CTAD). These modifications are not made under hypoxic conditions, allowing HIFα to accumulate and enter the nucleus where it associates with ARNT and binds to HREs upstream of hypoxia-activated genes. The red box highlights the HIFα and ARNT PAS-B domains. (*b*) Domain topology of HIFα subunits, including a bHLH domain, two PAS domains, and C-terminal regulatory domains. A sequence alignment of the HIFα PAS-B orthologs is shown, with bold letters indicating the mutated residues described in the text. HIF-2α PAS-B secondary structure elements are indicated with a gray background.

unless otherwise noted. ARNT PAS-B was expressed and purified as described in *Supporting Methods*, which is published as supporting information on the PNAS web site.

Parallel studies on human HIF-1α PAS-B used a construct containing residues 238–349, chosen by homology with HIF-2α PAS-B. Expression and purification of HIF-1α PAS-B were done as described for HIF-2α PAS-B.

NMR Spectroscopy. All NMR data were recorded at 30°C with Varian Inova 500 and 600 MHz spectrometers by using NMRPIPE for data processing (19) and NMRVIEW for analysis (20). Chemical-shift assignments were made by using standard methods (21) as detailed in *Supporting Methods*.

Deuterium exchange reactions were started by resuspending lyophilized ^{15}N-labeled HIF-2α PAS-B in 99% D_2O (uncorrected pH 7.3). These samples were then placed into a prewarmed magnet (T = 30°C), and ^{15}N/^{1}H heteronuclear sequential quantum correlation (HSQC) spectra were sequentially acquired approximately every 15 min. Observed ^{2}H exchange rates were converted into protection factors by using standard methods (22).

Structure Determination. Interproton distance constraints were obtained from 3D ^{15}N edited NOESY (τ_m = 150 ms), ^{15}N, ^{13}C edited NOESY (τ_m = 100 ms), and 2D NOESY (τ_m = 120 ms) spectra. Hydrogen bond constraints (1.3 Å < $d_{NH\text{-}O}$ < 2.5 Å, 2.3 Å < $d_{N\text{-}O}$ < 3.5 Å) were set for backbone amide protons protected for >30 min from exchange with D_2O solvent (30°C, pH 7.3). Constraints for the ϕ and ψ dihedral angles were generated by chemical-shift analyses by using TALOS (23), with two times the standard deviation of TALOS predictions as the bounds (minimum ± 30°). For 19 residues without TALOS predictions, ϕ dihedral angle constraints were obtained from an analysis of a 3D HNHA spectrum. Finally, 78 ^{15}N-^{1}H residual dipolar coupling constraints were obtained from a sample partially aligned in 5% (wt/vol) DMPC/DHPC ratio of 3:1 (Avanti Polar Lipids) and 5 mM cetyltrimethylammonium bromide at 35°C.

Initial structures were determined without manual assignments by using ARIA1.2 (24, 25) and subsequently refined with a mix of automated and manual assignment of NOESY spectra. Of 1,000 structures, the 20 lowest-energy structures were analyzed with MOLMOL (26) and PROCHECK-NMR (27).

From this ensemble, the structure closest to the mean was superimposed against other PAS domains with the DEEPVIEW Swiss Protein Data Bank program (28) with the automatic fit option. The calculated rms deviations ranged between 1.4 and 1.65 Å for HERG (Research Collaboratory for Structural Bioinformatics Protein Data Bank ID 1BYW), hPASK (1LL8), RmFixL (1D06), and Phy3 (1G28). The HIF-2α PAS-B structure was also used to generate a model of the HIF-1α PAS-B structure (74% sequence identity) by using MODELLER (29).

HIFα and ARNT PAS-B Titration. Titrations were conducted by the stepwise addition of natural abundance ARNT PAS-B (up to 800 μM) to a sample of 200-μM HIF-2α at 35°C. The peak heights of HIF-2α PAS-B signals that do not show ARNT-dependent chemical shift changes (38 residues) were fit to Eq. 1 to obtain the corresponding K_d:

$$\Delta I = 1 - \{\Delta I_{max} \times [(A + P_T + K_d) - ((A + P_T + K_d)^2 - (4 \times A \times P_T))^{1/2}]/[2 \times P_T]\}, \quad [1]$$

where ΔI is the observed change in peak height at ARNT concentration A, ΔI_{max} is the change in peak height at saturation, and P_T is the total HIFα concentration. Eq. 1 is similar to the equation used to extract K_d from chemical-shift changes observed in titrations of complexes undergoing fast exchange (30), and we apply it here only to sites without chemical-shift changes (fast exchange) to ensure that the observed peak line widths are a population-weighted average of the free- and bound-state line widths (31). The binding of HIF-2α PAS-B mutants to ARNT PAS-B was assessed by adding 900 μM natural abundant ARNT PAS-B to 250 μM HIFα PAS B at 25°C.

Mutagenesis. Point mutants of full-length HIF-1α and -2α were created from wild-type DNA and primers including the desired mutation(s). PAS-B domains containing these mutations were obtained by PCR amplification of the corresponding full-length sequence and subcloned into the pGβ1-parallel vector. Transformation, protein induction, and purification were performed as described above.

Transfections. Cells were plated onto 48-well plates (3.5×10^4 cells per well) in 200 μl of HyQ DME/F-12 1:1 media (HyClone) supplemented with 5% FBS 24 h before transfection. Cells were transfected with 10 ng of each HIFα construct and 20 ng of the 3HRE-tk-luc (HRE, hypoxia-responsive element) luciferase reporter construct (8) by using the Lipofectamine PLUS reagent (Invitrogen). After 3 h, the media were changed and, after an additional 2 h, cells were incubated for 15 h under normoxic or hypoxic (1.0% O_2) conditions. Luciferase activity was measured as described (32).

Results

Solution Structure of HIF-2α PAS-B. We determined the solution structure of HIF-2α PAS-B by using standard double- and triple-resonance NMR experiments conducted on uniformly ^{15}N and ^{15}N ^{13}C labeled protein samples (Fig. 2). This structure is

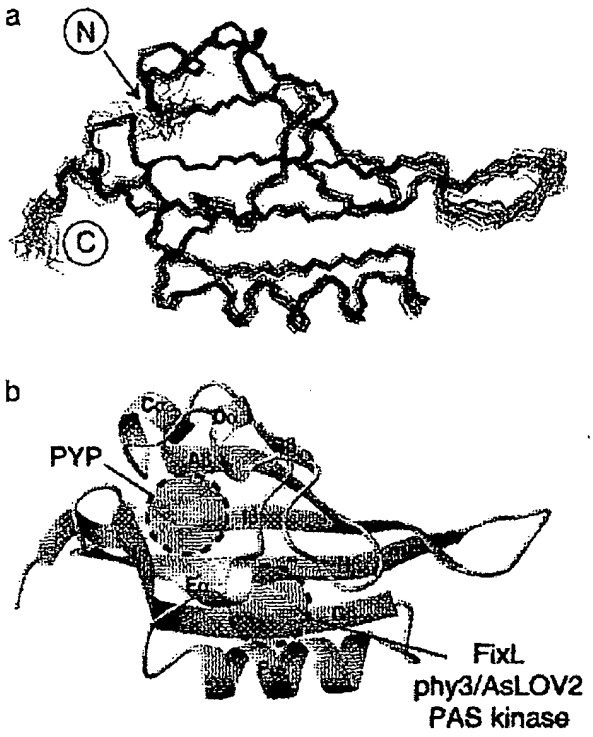

Fig. 2. Solution structure of HIF-2α PAS-B. (*a*) Superimposition of 20 lowest-energy structures for HIF-2α PAS-B, calculated as indicated in the text. (*b*) Ribbon diagram of the structure closest to the mean of the ensemble shown in *a*. Circles indicate the approximate locations of the ligand-binding sites of several PAS domains (17, 33–36).

Table 1. Statistics for HIF-2α PAS-B solution structure determination

List of constraints	
NOE distance restraints	
Unambiguous	2,767
Ambiguous	496
Hydrogen bond restraints	60
Dihedral angle restraints	96
^{15}N-^{1}H residual dipolar couplings	78
Stereospecific assignments (Val γ, Leu δ)	12
Structural analysis	
Mean rms deviation from experimental restraints	
NOE, Å	0.022 +/− 0.002
Dihedral angles, deg	1.04 +/− 0.16
Average number of:	
NOE violations >0.5 Å	0
NOE violations >0.3 Å	1.9 +/− 1.2
Dihedral violations >5°	1.6 +/− 1.1
Mean rms from idealized covalent geometry	
Bonds, Å	0.0045
Angles, deg.	0.65
Impropers, deg.	1.69
Geometric analysis of residues 6–91 and 98–112	
rms deviation to mean	0.53 +/− 0.07 Å (backbone)
	1.08 +/− 0.10 Å (all heavy)
Ramachandran analysis (PROCHECK)	81.0% most-favored
	16.4% additionally allowed
	1.6% generously allowed
	1.0% disfavored

based on >2,500 geometric constraints obtained from measurements of interproton distances, dihedral angles, and ^{15}N-^{1}H residual dipolar couplings of a partially oriented sample (Table 1). All of these data are well satisfied by the high-precision ensemble of the 20 lowest-energy structures subsequently used for further analysis.

HIF-2α PAS-B adopts a typical α/β PAS domain fold, characterized by several α-helices flanking a five-stranded antiparallel β sheet. The similarity of this structure to other PAS domains is demonstrated by the low-backbone rms deviation values (1.4–1.65 Å) of pairwise comparisons between representative PAS structures and HIF-2α PAS-B. Although several other PAS domains bind cofactors within their hydrophobic cores to regulate protein–protein interactions in response to various physical stimuli (11), a combination of NMR, mass spectrometry, and visible spectroscopy shows that HIF-2α PAS-B does not copurify with any such compound (data not shown). Further, no preformed cavities are present in the protein core, even at sites occupied by ligands in some other PAS domains (17, 33–36) (Fig. 2*b*).

Identification of ARNT PAS-B-Binding Surface on HIF-2α PAS-B. The PAS domains in bHLH-PAS transcription factors are thought to cooperate with the bHLH domains to facilitate dimerization (12, 13), which implies that the HIFα and ARNT PAS domains bind to each other (Fig. 1*a*). To experimentally demonstrate this interaction, we titrated unlabeled ARNT PAS-B into ^{15}N-labeled HIF-2α PAS-B and monitored changes in the HIF-2α ^{15}N/^{1}H HSQC spectrum (Fig. 3*a*). Peaks in these spectra showed both chemical-shift changes and line broadening on addition of ARNT PAS-B, consistent with binding on the intermediate and fast exchange time scales. In contrast, we found that HIF-2α PAS-B signals were not affected by the addition of a PAS domain from PAS kinase, a protein not involved in the hypoxia response (17) (data not shown), suggesting that the changes observed on addition of ARNT PAS-B reflect a specific HIF-2α/ARNT interaction.

The ARNT-induced changes in the HIF-2α line widths demonstrate two important effects. First, we observed a general increase in line width for HIF-2α peaks during the titration, which we attribute to the slower tumbling of the larger 27-kDa heterodimeric complex compared with an isolated HIF-2α PAS-B domain. By monitoring this broadening via the decrease in peak heights as ARNT PAS-B was added, we observed a titration consistent with a 1:1 binding event with a 30 μM K_d (Fig. 3*b*). This effect saturated at a 1:3 (HIF/ARNT) ratio, establishing that it is not caused by nonspecific increases in sample viscosity or aggregation. Second, we observed that a subset of residues preferentially broadened on the addition of substoichiometric amounts of ARNT PAS-B. Such differential effects have been observed in several complexes (17, 37, 38) and arise from exchange broadening at sites experiencing significant chemical-shift changes on complex formation. Mapping sites that exhibit either this differential broadening or significant ARNT-induced chemical shift changes onto the HIF-2α PAS-B structure shows that they cluster on the face of the central β-sheet (Fig. 4). This provides a chiefly hydrophobic surface for ARNT binding that is conserved among the HIF isoforms (Fig. 1), suggesting that the PAS-B domains of all three interact similarly with ARNT.

Evidence for the importance of this interface in the HIF/ARNT PAS-B dimer was obtained from studies of PAS-B domains containing point mutations. Based on our structure, we altered three

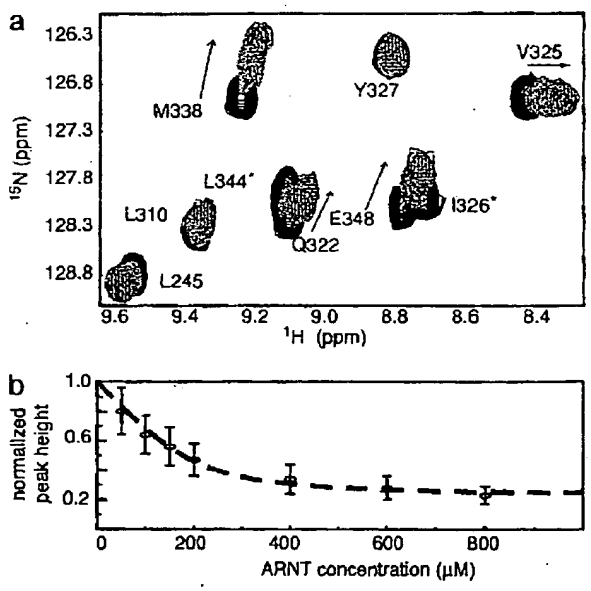

Fig. 3. Characterization of the HIF-2α/ARNT PAS-B-binding interaction. (a) Titration of unlabeled ARNT PAS-B (black, 0 μM; light blue, 200 μM; blue, 600 μM; red, 800 μM ARNT) into a 200 μM ^{15}N-labeled HIF-2α PAS-B solution. Arrow shows direction of peak shifts with increasing amounts of ARNT. Residues with peak broadening beyond detection during the titration are indicated with *. (b) Normalized peak heights of HIF-2α PAS-B (38 resonances) plotted against increasing amounts of ARNT PAS-B. The concentration dependence of the observed reduction in peak heights can be fit to a 1:1 binding event with a K_d of ~30 μM (dotted line).

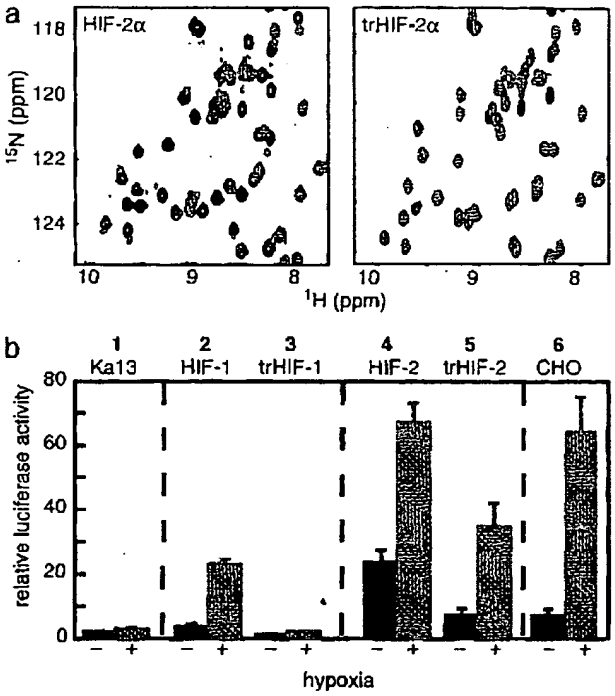

Fig. 5. Point mutations in the HIFα PAS-B central β-sheet disrupt the binding of ARNT PAS-B. (a) Superimposed ^{15}N/^{1}H HSQC spectra of 250 μM ^{15}N labeled HIF-2α PAS-B (*Left*) or triple mutant (Q322E/M338E/Y342T) (*Right*). Spectra in the presence of 900 μM unlabeled ARNT PAS-B are shown with red contours; those without ARNT are shown in black contours. Similar data for HIF-1α PAS-B are provided in *Supporting Methods*. (b) PAS-B domain interaction is important to form a biologically active HIF/ARNT complex. A construct expressing a luciferase reporter under the control of an HRE promoter was transfected into Ka-13 (columns 1–5) or CHO (column 6) cells along with various HIFα constructs. Values represent the average luciferase activity of three samples, with bars indicating standard error. Luciferase expression was induced by cotransfection of HIF-1α (column 2) or HIF-2α (column 4), particularly under hypoxic conditions. Cotransfection of trHIF-1α (column 3) or trHIF-2α (column 5), full-length HIFα proteins containing the three PAS-B mutations, shows a significant drop in luciferase activity compared with wild-type HIFα.

residues with solvent-exposed side chains within the Hβ and Iβ strands (Q322E, M338E, and Y342T) (Fig. 4*b*). ^{15}N/^{1}H HSQC spectra of this triple mutant (trHIF-2α PAS-B) retain the chemical-shift dispersion and general pattern of the wild-type protein, confirming that the protein structure remains intact (Fig. 5*a*). The ARNT-binding capability of this mutant was assessed by comparing ^{15}N/^{1}H HSQC spectra before and after addition of unlabeled ARNT PAS-B. As demonstrated by the minimal ARNT-induced changes in peak locations and intensities, the interaction of the triple mutant HIF-2α PAS-B with ARNT has been very significantly weakened. These data establish that subtle changes on the surface of the Hβ and Iβ strands of HIF-2α PAS-B can disrupt the HIF–ARNT PAS-B interaction.

Comparison of HIF-1α and -2α PAS-B. Sequence alignments of HIF-1α and -2α indicate that the PAS-B domains of these proteins are extremely similar (74% identity; Fig. 1*b*). Nevertheless, the HIF-1α homolog of our HIF-2α PAS-B construct

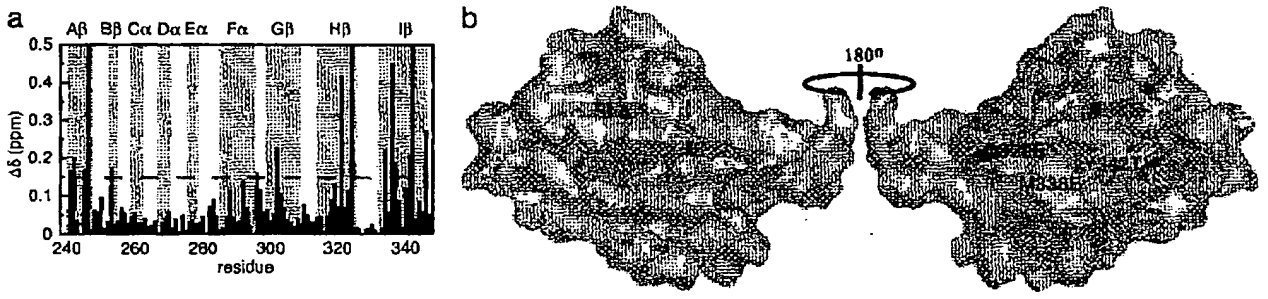

Fig. 4. Identification of the ARNT PAS-B-binding site on the surface of HIF-2α PAS-B. (a) Chemical-shift changes from ^{15}N/^{1}H HSQC spectra of HIF-2α PAS-B in the presence of 800 μM ARNT are plotted as a function of residue number. The red line indicates chemical-shift changes >0.16 ppm. Residues with peak broadening beyond detection are shown as an arbitrary chemical-shift change of 0.5 ppm. Secondary structure elements are indicated with a gray background. (b) Surface representations of HIF-2α PAS-B showing the location of the ARNT PAS-B-binding site. Colors indicate residues with large chemical-shift changes (>0.4 ppm) or broadening beyond detection (red), residues with a significant chemical-shift changes (>0.16 ppm) (orange), and the site of the mutated residues that disrupt the HIF/ARNT PAS-B interactions (yellow). Figs. 4 and 6 were made with PYMOL (www.pymol.org).

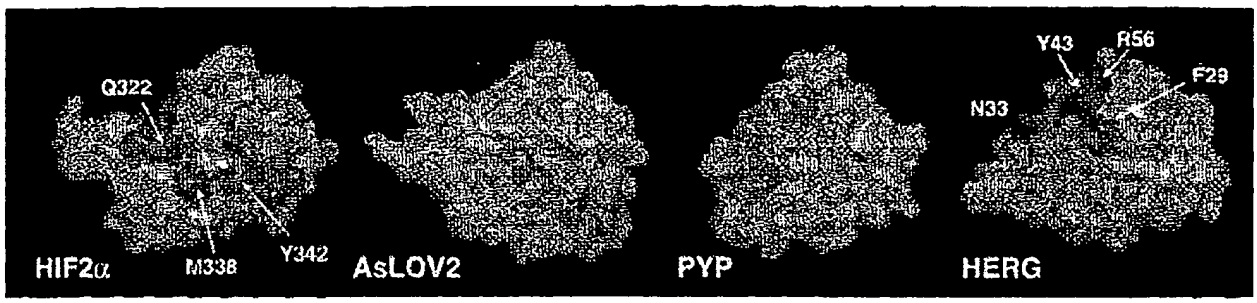

Fig. 6. Versatility of protein interactions involving PAS domain β-sheets. HIF2α is shown in the same orientation as Fig. 4*b* and colored by residues experiencing significant $^{15}N/^{1}H$ chemical shifts on complex formation (red) and those used to generate the complex-disrupting trHIF-2α (blue). Phototropin (AsLOV2) (36) and photoactive yellow protein (33) highlight the α-helices external to the PAS core (magenta) and any atoms located within 5 Å of those helices (pink). HERG (42) shows functionally important, solvent-exposed residues (dark blue) and residues present in a surface hydrophobic patch suggested to be important for channel function (light blue) (42).

was too poorly behaved in solution to be amenable to structure determination. However, by combining the high sequence identity between these PAS-B domains and the HIF-2α PAS-B solution structure, we generated a homology model of HIF-1α PAS-B (29). This guided our mutation of three solvent-exposed residues in the HIF-1α PAS-B β-sheet (Q320E/V336E/Y340T) at sites analogous to those changed in HIF-2α PAS-B. Interestingly, this HIF-1α PAS-B triple mutant was significantly better behaved in solution than the wild-type domain. To determine whether HIF-1α PAS-B bound ARNT PAS-B in a similar fashion as HIF-2α PAS-B, we recorded $^{15}N/^{1}H$ HSQC of wild-type and triple-mutant HIF-1α PAS-B in the presence and absence of ARNT PAS-B (Fig. 7, which is published as supporting information on the PNAS web site). In the case of wild-type HIF-1α PAS-B, the combination of specific peak shifting and line broadening on the addition of ARNT PAS-B indicated binding. In contrast, this interaction was disrupted in the triple mutant (Fig. 7), demonstrating that the interface identified in HIF-2α is as crucial for the ARNT-binding function of HIF-1α.

Functional Importance of PAS-B in Full-Length HIFα. Our demonstration of specific interactions between the isolated HIFα and ARNT PAS-B domains suggested that they function as dimerization elements in the HIF heterodimer. To address this question in living cells with full-length HIFα, we used a luciferase-based assay that uses Chinese hamster ovary (CHO) cells lacking functional HIFα (CHO-Ka13) (39). CHO-Ka13 cells were transiently transfected with full-length HIFα constructs under the control of the HIF-1 promoter (40) and encoding either wild-type or a mutant sequence containing the three PAS-B domain mutations. Low levels of DNA were transfected to roughly match the HIF activity in wild-type CHO cells. The abilities of these HIFα constructs to activate transcription were determined by measuring the expression of luciferase under the control of a minimal HRE promoter (8).

After expressing either wild-type HIF-1α or -2α, the hypoxia response of the transfected CHO-Ka13 cells mimicked that of wild-type CHO cells, confirming that HIFα activity can be rescued by expression from these plasmids (Fig. 5*b*). Cells transfected with HIF-2α constructs either lacking the entire PAS-B domain (Δ240–350) or containing a mutation known to unfold PAS-B (C339P; unfolded as established by NMR) showed no significant luciferase activity under any conditions (data not shown). Although these results suggest that HIFα PAS-B plays a crucial role in forming a biologically active HIFα/ARNT heterodimer, the question remained whether the subtler PAS-B modifications that disrupted *in vitro* binding would have a similar effect. Therefore, we transfected CHO-Ka13 cells with full-length HIF-1α and -2α constructs containing the three PAS-B mutations (trHIFα). For both mutant proteins, the HRE-driven luciferase response is decreased compared with that observed in cells containing vectors expressing wild-type HIFα. In the case of trHIF-1α, the response is virtually eliminated (Fig. 5*b*, column 3), whereas a less pronounced but significant reduction is observed for trHIF-2α (Fig. 5*b*, column 5). These results are surprising in light of the three apparently redundant sets of protein–protein interactions implied by the model of the HIF heterodimer (Fig. 1*a*). Our data show that the subtle disruption of the PAS-B interaction within the full length HIFα protein is sufficient to prevent the formation of the HIF transcription factor, thereby abolishing the hypoxia response.

Discussion

Despite the intense interest in hypoxia signaling, previous understanding of the roles of various protein–protein interactions in the HIF heterodimer remained unclear. Much of the data underlying prior work in this area were based on deletions generated at a time when the lack of structural data hampered the design of constructs cleanly corresponding to PAS domain boundaries. Unfortunately, this approach has complicated the interpretation of these findings with respect to the functional importance of individual PAS domains. In this context, our results provide the structural insight to clarify how PAS-B domains contribute to the stability of HIF and other bHLH-PAS transcription factor complexes. We demonstrate that the PAS-B domains of HIFα and ARNT directly associate *in vitro*, using a group of predominantly hydrophobic residues located on the solvent-exposed face of the HIFα β-sheet. Critically, mutations that disrupt the interaction between isolated PAS-B domains *in vitro* also interfere with the ability of the full-length heterodimer to activate transcription in living cells. These results establish the importance of the β-sheet interaction surface of HIFα PAS-B domains within the complexes that are central to the hypoxia response pathway.

More broadly, the β-sheet interface we identified appears to be important for a wide array of inter- and intramolecular interactions within several PAS domains (Fig. 6). Evidence of this commonality is provided by PAS domains from two blue-light photoreceptors, phototropin1 (AsLOV2) (36) and photoactive yellow protein (33). Both of these domains are flanked by additional α-helical elements that fold back on the PAS domain itself, associating with the same β-sheet region used by HIFα to bind ARNT (Fig. 6). An additional example is provided by the human ether-a-go-go-related gene (HERG) potassium channel, which contains a PAS domain that controls the poststimulation deactivation kinetics of this channel, possibly by interacting with

the S4-S5 linker (41). Point mutations in the PAS domain that impair channel function have been identified by both alanine scanning mutagenesis (42) and sequencing of HERG genes from individuals affected by long QT syndrome (41), an inherited cardiac disorder associated with defects in HERG and other ion channels. Biochemical studies of channels containing one of several conservative mutations in solvent-exposed residues (F29L, F29A, N33T, Y43A, and R56Q; Fig. 6) demonstrate that the region analogous to the HIF/ARNT interface plays an important role in regulating HERG channel kinetics. In summary, these comparisons indicate that the exposed face of the central β-sheet in PAS domains is well suited for making many functionally important types of associations.

This comparison also suggests a route that might be exploited to regulate the formation of the HIFα–ARNT complex by using small organic compounds. Although neither a natural ligand nor a ligand-binding cavity has been identified for the HIFα PAS-B domains, this should not be interpreted to mean this domain cannot bind any small compounds. Indeed, it has been demonstrated that certain artificial chemicals can specifically bind into the well packed hydrophobic core of a PAS domain from PAS kinase (Fig. 2*b*) (17), likely producing significant conformational changes therein. Parallel studies of two PAS domains with natural cofactors, AsLOV2 and photoactive yellow protein, have shown that relatively small structural changes in these internally bound compounds are sufficient to displace α-helices bound onto the same β-sheet interface we identified in HIFα (36, 43). Combining these observations and an earlier model proposed for PAS domain signaling (44) raises the possibility that binding compounds in the HIFα PAS-B core could generate structural changes that disrupt the interactions needed to form the HIF heterodimer, analogous to the HIFα mutations demonstrated here. Given the central role of HIF in the hypoxia response and the importance of this pathway in cancer progression, this approach may serve as the basis for a novel therapeutic strategy (1, 2).

We thank M. Rhima for technical assistance; P. Ratcliffe (Oxford University, Oxford) for the gift of the Ka13 cell line; and D. Russell, J. Garcia, and S. McKnight for comments on the manuscript. This work was supported by grants from the National Institutes of Health (CA90601 to K.H.G. and CA95471 to K.H.G. and R.K.B.), the University of Texas Southwestern Endowed Scholars Program (to K.H.G. and R.K.B.), and the Robert A. Welch Foundation (I-1424 to K.H.G.). P.B.C. was supported by a National Institutes of Health Training Grant GM08297 to the University of Texas Southwestern Graduate Program in Molecular Biophysics. R.K.B. is supported by a Career Award in the Biomedical Sciences from the Burroughs Wellcome Fund.

1. Semenza, G. L. (2000) *Genes Dev.* **14**, 1983–1991.
2. Ratcliffe, P. J., Pugh, C. W. & Maxwell, P. H. (2000) *Nature* **6**, 1315–1340.
3. Wang, G., Jiang, B., Rue, E. & Semenza, G. (1995) *Proc. Natl. Acad. Sci. USA* **92**, 5510–5514.
4. Min, J. H., Yang, H., Ivan, M., Gertler, F., Kaelin, W. G., Jr., & Pavletich, N. P. (2002) *Science* **296**, 1886–1889.
5. Dames, S. A., Martinez-Yamout, M., De Guzman, R. N., Dyson, H. J. & Wright, P. E. (2002) *Proc. Natl. Acad. Sci. USA* **99**, 5271–5276.
6. Freedman, S. J., Sun, Z. Y., Poy, F., Kung, A. L., Livingston, D. M., Wagner, G. & Eck, M. J. (2002) *Proc. Natl. Acad. Sci. USA* **99**, 5367–5372.
7. Semenza, G. L. (1999) *Annu. Rev. Cell Dev. Biol.* **15**, 551–578.
8. Tian, H., McKnight, S. & Russell, D. (1997) *Genes Dev.* **11**, 72–82.
9. Gu, Y.-Z., Moran, S. M., Hogenesch, J. B., Wartman, L. & Bradfield, C. A. (1998) *Genes Dev.* **7**, 205–213.
10. Massari, M. E. & Murre, C. (2000) *Mol. Cell. Biol.* **20**, 429–440.
11. Taylor, B. L. & Zhulin, I. B. (1999) *Microbiol. Mol. Biol. Rev.* **63**, 479–506.
12. Pongratz, I., Antonsson, C., Whitelaw, M. L. & Poellinger, L. (1998) *Mol. Cell. Biol.* **18**, 4079–4088.
13. Hogenesch, J. B., Chan, W. K., Jackiw, V. H., Brown, R. C., Gu, Y.-Z., Pray-Grant, M., Perdew, G. H. & Bradfield, C. A. (1997) *J. Biol. Chem.* **272**, 8581–8593.
14. Jiang, B.-H., Rue, E., Wang, G. L., Roe, R. & Semenza, G. L. (1996) *J. Biol. Chem.* **271**, 17771–17778.
15. Gradin, K., McGuire, J., Wenger, R., Kvietikova, I., Whitelaw, M., Toftgard, R., Tora, L., Gassmann, M. & Poellinger, L. (1996) *Mol. Cell. Biol.* **16**, 5221–5231.
16. Sheffield, P., Garrard, S. & Derewenda, Z. (1999) *Protein Expr. Purif.* **15**, 34–39.
17. Amezcua, C. A., Harper, S. M., Rutter, J. & Gardner, K. H. (2002) *Structure (Cambridge, U.K.)* **10**, 1349–1361.
18. Erbel, P. J. A., Barr, K., Gao, N., Gerwig, G. J., Rick, P. D. & Gardner, K. H. (2003) *J. Bacteriol.* **185**, 1995–2004.
19. Delaglio, F., Grzesiek, S., Vuister, G. W., Zhu, G., Pfeifer, J. & Bax, A. (1995) *J. Biomol. NMR* **6**, 277–293.
20. Johnson, B. A. & Blevins, R. A. (1994) *J. Biomol. NMR* **4**, 603–614.
21. Sattler, M., Schleucher, J. & Griesinger, C. (1999) *Prog. NMR Spectrosc.* **34**, 93–158.
22. Bai, Y., Milne, J. S., Mayne, L. & Englander, S. W. (1993) *Proteins* **17**, 75–86.
23. Cornilescu, G., Delaglio, F. & Bax, A. (1999) *J. Biomol. NMR* **13**, 289–302.
24. Brünger, A. T., Adams, P. D., Clore, G. M., Delano, W. L., Gros, P., Grosse-Kunstleve, R. W., Jiang, J. S., Kuszewski, J., Nilges, M. & Pannu, N. S. (1998) *Acta Crystallogr. D* **54**, 905–921.
25. Nilges, M. & O'Donoghue, S. I. (1998) *Prog. NMR Spectrosc.* **32**, 107–139.
26. Koradi, R., Billeter, M. & Wüthrich, K. (1996) *J. Mol. Graphics* **14**, 51–55.
27. Laskowski, R. A., Rullman, J. A. C., MacArthur, M. W., Kaptein, R. & Thornton, J. M. (1996) *J. Biomol. NMR* **8**, 477–486.
28. Gucx, N., and Peitsch, M. C. (1997) *Electrophoresis* **18**, 2714–2723.
29. Marti-Renom, M. A., Stuart, A., Fiser, A., Sanchez, R., Melo, F. & Sali, A. (2000) *Annu. Rev. Biophys. Biomol. Struct.* **29**, 291–325.
30. Dalvit, C., Flocco, M., Knapp, S., Mostardini, M., Perego, R., Stockman, B. J., Veronesi, M. & Varasi, M. (2002) *J. Am. Chem. Soc.* **124**, 7702–7709.
31. Pulmer, A. G., III, Kroenke, C. D. & Loria, J. P. (2001) *Methods Enzymol.* **339**, 204–238.
32. Bruick, R. K. (2000) *Proc. Natl. Acad. Sci. USA* **97**, 9082–9087.
33. Borgstahl, G. E. O., Williams, D. R. & Getzoff, E. D. (1995) *Biochemistry* **34**, 6278–6287.
34. Crosson, S. & Moffat, K. (2001) *Proc. Natl. Acad. Sci. USA* **98**, 2995–3000.
35. Gong, W., Hao, B., Mansy, S. S., Gonzalez, G., Gilles-Gonzalez, M. A. & Chan, M. K. (1998) *Proc. Natl. Acad. Sci. USA* **95**, 15177–15182.
36. Harper, S. M., Neil, L. C. & Gardner, K. H. (2003) *Science* **301**, 1541–1544.
37. Sette, M., van Tilborg, P., Spurio, R., Kaptein, R., Paci, M., Gualerzi, C. O. & Boelens, R. (1997) *EMBO J.* **16**, 1436–1443.
38. Matsuo, H., Walters, K. J., Teruya, K., Tanaka, T., Gassner, G. T., Lippard, S. J., Kyogoku, Y. & Wagner, G. (1999) *J. Am. Chem. Soc.* **121**, 9903–9904.
39. Woot, S. M., Wiesener, M. S., Yeates, K. M., Okada, N., Pugh, C. W., Maxwell, P. H. & Ratcliffe, P. J. (1998) *J. Biol. Chem.* **273**, 8360–8368.
40. Minet, E., Ernest, I., Michel, G., Roland, I., Remacle, J., Raes, M. & Michiels, C. (1999) *Biochem. Biophys. Res. Commun.* **261**, 534–540.
41. Chen, J., Zou, A., Splawski, I., Keating, M. T. & Sanguinetti, M. C. (1999) *J. Biol. Chem.* **274**, 10113–10118.
42. Morais Cabral, J. H., Lee, A., Cohen, S. L., Chait, B. T., Li, M. & Mackinnon, R. (1998) *Cell* **95**, 649–655.
43. Hoff, W. D., Xie, A., Van Stokkum, I. H. M., Tang, X. J., Gural, J., Kroon, A. R. & Hellingwerf, K. J. (1999) *Biochemistry* **38**, 1009–1017.
44. Cusanovich, M. A. & Meyer, T. E. (2003) *Biochemistry* **42**, 4759–4770.

RECEIVED
CENTRAL FAX CENTER
MAR 19 2007

IN THE UNITED STATES PATENT AND TRADEMARK OFFICE

Serial No. 10/677,734	Customer No. 23379
Applicant: Gardner et al.	Confirmation No. 4912
Filed: Oct 01, 2003	Group Art Unit: 1656
Docket No. UTSD:1510-1	Examiner: Swope, Sheridan

Title: *Foreign PAS Ligands Regulate PAS Domain Function*

DECLARATION UNDER 37CFR1.132

I, Professor Stephen R. Sprang, declare and state as follows:

1. I am a Professor in the Department of Biochemistry at the University of Texas Southwestern Medical School. The Board of Regents of the University of Texas System is the assignee of this patent application. I have authored numerous scientific papers in the field of protein regulation, and I am familiar with this patent application. A copy of my curriculum vitae is attached.

2. HIF2α PAS B domain is an art-recognized, defined protein domain, and one skilled in the art does not require undue effort or experimentation to recognize and procure an HIF2α PAS B domain for use in the claimed methods, as documented for example by Erbel *et al.*, *Proc. Natl. Acad. Sci.* **100**(2003): 15504-9. In my opinion the Specification enables one skilled in the art to practice the invention without undue experimentation.

3. HIF2α PAS B domain is an art-recognized, defined protein domain, and one skilled in the art has no trouble recognizing an HIF2α PAS B domain for use in the claimed methods. There are many scientific publications describing the HIF2α PAS B domain, and how to use it (e.g. Erbel *et al.*, 2003, supra). In my opinion the specification amply describes and exemplifies the claimed methods to one skilled in the art.

4. Vogtherr (2003) generally describes the use of NMR-based screening for lead discovery; Amezcua (2002) describes the used of NMR to detect ligand binding to PAS kinase; Ema (1997) reports that *HIF1a* heterodimerizes with ARNT (note that HIF1α is structurally and functionally distinct from the recited HIF2α; Sowter *et al.*, *Cancer Res.* **63**(2003): 6130-4 and Raval *et al.*, *Mol Cell Biol* **25**(2005): 5675-86); and Fukunaga (1995) reports identification of functional domains of the aryl hydrocarbon receptor.

Prior to the present disclosure, HIF was known to be regulated in several ways by oxygen availability, but only via mechanisms that are based on oxygen-sensitive enzymes that covalently modify portions of the HIFα subunit at sites distant to the PAS domains (Bruick & McKnight,

Science **294**(2001): 1337-40; Jaakkola et al, *Science* **292**(2001): 468-72; Ivan *et al., Science* **292**(2001): 464-8; Lando *et al.*, *Science* **295**(2002): 858-61). These findings demonstrated two independent modes of oxygen regulation that do not involve the PAS domains, which taught away from any expectation that the HIF PAS domains would be sensory.

In addition, HIF2α PASB presents a well-folded domain, which significantly contrasts with the dynamic regions of PASK PAS A (Amezcua *et al.*, *Structure* **10**(2002): 1349-61; Erbel *et al.*, 2003, supra), further removing any expectation of core ligand binding. Indeed, the structure of the ligand-free [apo] form of HIF2α PASB is in contrast with the apo-structures of the many small ligand-binding protein domains, which either exhibit pre-formed cavities or pockets for ligands to bind or alternatively adopt an unfolded (and often, chaperone-bound) conformation. The HIF2α PAS B structure shows neither of these.

Based on what was known prior to this disclosure, it is my opinion that one skilled in the art at the time of the filing date would not have expected HIF2α PAS to provide a core for sensory ligand binding.

I hereby declare that all statements made herein of my own knowledge are true and that all statements made on information and belief are believed to be true; and further that these statements are made with the knowledge that willful false statements and the like so made are punishable by fine or imprisonment, or both, under Section 1001 of Title 18 of the United States Code and that such willful, false statements may jeopardize the validity of the application and any patent issuing therefrom.

Date: June 19 2006

Professor Stephen R. Sprang

[CANCER RESEARCH 63, 6130–6134, October 1, 2003]

Advances in Brief

Predominant Role of Hypoxia-Inducible Transcription Factor (Hif)-1α *versus* Hif-2α in Regulation of the Transcriptional Response to Hypoxia[1]

Heidi M. Sowter, Raju Raval, John Moore, Peter J. Ratcliffe, and Adrian L. Harris[2]

Cancer Research UK, Weatherall Institute of Molecular Medicine, John Radcliffe Hospital, Oxford OX3 9DU [H. M. S., J. M., A. L. H.], and Wellcome Trust Centre for Human Genetics, Oxford OX3 7BN [R. R., P. J. R.], United Kingdom

Abstract

Tumor hypoxia induces the up-regulation of a gene program associated with angiogenesis, glycolysis, adaptation to pH, and apoptosis via the hypoxia-inducible transcription factors (Hifs) 1 and 2. Disruption of this pathway has been proposed as a cancer therapy. Here, we use short interfering RNAs to compare specific inactivation of Hif-1α or Hif-2α and show markedly different cell type-specific effects on gene expression and cell migration. Remarkably, among a panel of hypoxia-inducible genes, responses were critically dependent on Hif-1 α but not Hif-2 α in both endothelial and breast cancer cells but critically dependent on Hif-2 α in renal carcinoma cells.

Introduction

Hypoxia is an important process in the progression and treatment resistance of many human cancers (1). The majority of human cells share a common mechanism of oxygen sensing mediated by Hifs[3] 1 and 2. These proteins are heterodimers consisting of α subunits, Hif-1α and Hif-2α (also known as endothelial PER-ARNT-SIM domain protein 1) that dimerize with the constitutively expressed aryl hydrocarbon receptor nuclear translocator (also known as Hif-1β; reviewed in Ref. 2). Both Hif-α molecules are subject to similar regulatory processes involving enzymatic hydroxylation of conserved prolyl and asparaginyl residues that target them for degradation via the VHL ubiquitin E3 ligase complex (reviewed in Ref. 3). Moreover, in transfection assays, both transcription factors activate a range of hypoxia response elements with similar efficacy (4, 5).

Despite these striking similarities, genetic studies have provided firm evidence for nonredundant functions. Targeted inactivation of Hif-1α and Hif-2α in embryonic stem cells is associated with different patterns of response to hypoxia and low glucose stress (6), and different developmental defects are observed in Hif-1$\alpha^{-/-}$ and Hif-2$\alpha^{-/-}$ mouse embryos (for review see Ref. 3). In part, differences may relate to distinct patterns of cellular expression. For instance, in the kidney, whereas both transcription factors are abundantly expressed, Hif-1α is the predominant form in epithelial cells, whereas Hif-2α is predominant in interstitial fibroblast and endothelial cells (7). However, many cancers and cell lines express both isoforms. The expression of the two Hif-α isoforms at similar levels in this setting might be predicted to lead to a level of redundancy. Nevertheless, overexpression of Hif-2α, but not Hif-1α, promoted growth of renal cell carcinoma cells (8, 9) yet inhibited growth of breast cells (10), suggesting distinct effects on biology. These findings raise important questions as to what extent Hif-1α and Hif-2α have overlapping or redundant transcriptional functions in the cancer setting, whether expression of particular Hif transcriptional targets are always linked to expression of a particular Hif-α isoforms, or whether transcriptional selectivity varies according to cell background.

We have used siRNAs to specifically inhibit Hif-1α and Hif-2α production in human breast and renal carcinoma cell lines and in a human endothelial cell line, which express differing levels of Hif-1α and Hif-2α, ranging from isolated expression of Hif-1α to isolated expression of Hif-2α. The role of each molecule on induction of specific transcriptional targets with a variety of functions in the hypoxic response was then investigated.

Materials and Methods

siRNA Duplexes. The siRNA oligonucleotides were designed after the recommendations of Elbashir *et al.* (11) and were synthesized and high-performance liquid chromatography purified at Transgenomic Laboratories (Glasgow, United Kingdom). The Hif-1α siRNA duplex targeted nucleotides 1521–1541 of the Hif-1α mRNA sequence (NM001530) and comprised of: sense 5′-CUGAUGACCAGCAACUUGAdTdT-3′ and antisense 5′-UCAAGUUGCUGGUCAUCAGdTdT-3′. The Hif-2α siRNA duplex targeted nucleotides 1260–1280 of the Hif-2α mRNA sequence (NM001430) and comprised of sense 5′-CAGCAUCUUUGAUAGCAGUdTdT-3′ and antisense 5′-ACUGCUAUCAAAGAUGCUGdTdT-3′. The inverted Hif-1α control duplex did not target any gene and comprised of sense 5′-AGUUCAACGACCAGUAGUCdTdT-3′ and antisense 5′-GACUACUGGUCGUUGAdTdT-3′. Duplexes were prepared by mixing 50-μM concentrations of antisense and sense oligonucleotides with annealing buffer [30 mM HEPES (pH 7.0), 100 mM potassium acetate, and 2 mM magnesium acetate], heat denaturing for 1 min at 85°C, and annealing at 37°C for 1 h. Duplex formation was confirmed by electrophoresis through 5% low melting temperature agarose (NuSieve GTG; FMC Bioproducts, Rockland, ME). Additional siRNA duplexes used for confirmation of the specificity of particular effects were prepared as above and targeted to nucleotides 1510–1530 (AACGACACAGAAACTGATGAC) of the Hif-1α mRNA sequence and nucleotides 328–348 (AAATCAGCTTCCTGCGAACAC) of the Hif-2α mRNA sequence.

Cell Culture. MDA 435 cells, MDA 468 cells (breast cancer), 786-0 cells (renal cancer), and HUVECs (endothelial) were obtained from the Cancer Research United Kingdom cell service. Breast and renal cancer cells were grown in DMEM supplemented with 10% FCS (Globepharm), L-glutamine (2 μM), penicillin (50 IU/ml), and streptomycin sulfate (50 μg/ml). HUVECs were grown in the media supplemented as above but with 20% FCS plus endothelial cell growth supplement and heparin (Sigma) and grown on plates coated with 2% gelatin/PBS. Experiments were performed on dishes of cells in normoxia (humidified air with 5% CO_2) or hypoxia [hypoxic conditions were generated in a Napco 7001 incubator (Precision Scientific) with 0.1% O_2, 5% CO_2, and balance N_2].

siRNA Treatment of Cells. Cells were plated onto 10-cm^2 cell culture dishes and grown to 30–50% confluence before transfection. The duplexes were diluted to give a final concentration of 20 nM in Opti-Mem I (Invitrogen life Technologies, San Diego, CA). Twenty-five μl of Oligofectamine transfection reagent (Invitrogen Life Technologies) were added, and the mixture

Received 7/7/03; revised 8/12/03; accepted 8/15/03.

The costs of publication of this article were defrayed in part by the payment of page charges. This article must therefore be hereby marked *advertisement* in accordance with 18 U.S.C. Section 1734 solely to indicate this fact.

[1] H. M. S., J. M. and A. L. H. were funded by Cancer Research United Kingdom and P. J. R. by the Wellcome Trust. R. R. is a Rhodes scholar.

[2] To whom requests for reprints should be addressed, at Weatherall Institute of Molecular Medicine, John Radcliffe Hospital, Oxford OX3 9DU, United Kingdom. Phone: 44-1865-222457; Fax: 44-1865-222431; E-mail: harrisa@cancer.org.uk.

[3] The abbreviations used are: Hif, hypoxia-inducible factor; CA9, carbonic anhydrase 9; Glut-1, glucose transporter-1; HUVEC, human umbilical vein endothelial cell; siRNA, short interfering RNA; uPAR, urokinase-type plasminogen activator receptor; VEGF, vascular endothelial growth factor; VHL, von Hippel-Lindau.

incubated at room temperature for 25 min. The cells were rinsed with Opti-Mem I to remove any residual serum and incubated with the oligonucleotide duplexes in serum-free conditions for 4 h at 37°C. Serum was then added back to the culture, and cells were incubated for an additional 24 h before beginning an experiment.

RNA Preparation and RNase Protection Assay. Cells were rinsed with PBS and drained thoroughly. RNA was extracted from the cells using the solution D method described by Chomczynski and Sacchi (12) and assessed by absorbance at 260/280 nm. The RNase protection assay protocol and generation of ^{32}P-labeled RNA probes to Hif-1α, Hif-2α, and U6 small nuclear RNA has been described previously (4). Protected fragments were resolved on an 8% polyacrylamide gel and analyzed on a PhosphorImager (Molecular Dynamics, Sunnyvale, CA).

Western Blotting. Cells were washed thoroughly with PBS before being homogenized in a lysis buffer containing 8 M urea, 10% SDS, 1 M DTT, and protease inhibitors. Samples were electrophoresed on a 10% SDS-PAGE gel and transferred onto a polyvinylidene difluoride membrane (Millipore, Bedfordshire, United Kingdom). Proteins were detected using monoclonal antibodies to Hif-1α (Signal Transduction Laboratories), Hif-2α (4), CA9 (13), GLUT-1 (Alpha Diagnostic, San Antonio, TX), glyceraldehyde-3-phosphate dehydrogenase (Abcam, Cambridge, United Kingdom), and BNip3 (14) at 1:1,000, 1:1,000, 1:500, 1:250, 1:2,000, and 1:20,000, respectively. As a loading control, a mouse monoclonal antibody to β-tubulin (Sigma) was used at 1:20,000. Overnight primary antibody incubation was followed by incubation with goat antimouse or rabbit horseradish peroxidase (Dako) and enhanced chemiluminescence developing reagents (Amersham). Blots were exposed to film for between 30 s and 2 min.

Measurement of VEGF and uPAR. Supernatant was harvested from treated cells and centrifuged to remove cell debris. Secreted VEGF and uPAR were measured in the supernatant using the respective Quantikine ELISA kit (R&D Systems, Abingdon, United Kingdom) as per the manufacturer's instructions. The amount of VEGF and uPAR in the supernatant was normalized to the final number of cells in the dish from which it was harvested.

Cell Migration Assay. Cells treated with siRNA as described above were incubated in 0.1% oxygen for 16 h, removed from the culture dish using 2 mM EDTA, and resuspended in 1% FCS media. A total of 200 μl of serum-free media containing 1.5×10^4 cells was placed into the top of migration chambers with 8-μm filters (24-well plate format; Falcon), which were standing in wells containing 700 μl of media containing 10% FCS. The cells were incubated at 37°C for 4 h, after which the chambers were removed from the wells and coded for analysis by a blinded observer. Cells that had migrated to the bottom of the filter were fixed with 2.5% glutaraldehyde for 15 min, rinsed thoroughly with PBS, and stained with 0.1% crystal violet for 2 min. The total number of cells on the bottom of each filter was counted under a microscope, and each experiment was performed in triplicate on at least three occasions.

Results

Specificity of siRNAs Targeted to Hif-1α and Hif-2α. We synthesized siRNA oligonucleotides that specifically target Hif-1α or Hif-2α mRNAs for degradation and transfected these into cells 24 h before hypoxic stimulation. RNA extracted from the treated cells was subjected to RNAse Protection Assay analysis for Hif-1α and Hif-2α. MDA 468 and HUVECs expressed transcripts encoding both Hif-1α and Hif-2α (Fig. 1), whereas the MDA 435 cells did not express Hif-2α mRNA (Fig. 1), and the 786-0 cells did not express Hif-1α mRNA (Fig. 1). Treatment of the cells with the siRNAs ablated the expression of Hif-1α and Hif-2α mRNA specifically in that the Hif-1α siRNA did not affect the Hif-2α gene expression and *vice versa* (Fig. 1). Inverted siRNA controls of the Hif-1α and Hif-2α siRNAs had no effect on the expression of either gene; the inverted Hif-1α siRNA was used as the control in all experiments described (Figs. 1–4). When cells were transfected with both siRNAs, expression of Hif-1α and Hif-2α was ablated. No cell toxicity was noted after transfection with either of the siRNAs or with Oligofectamine alone (described as the negative control). To confirm the specificity of the technique, siRNAs targeted to another region of the Hif-1α and

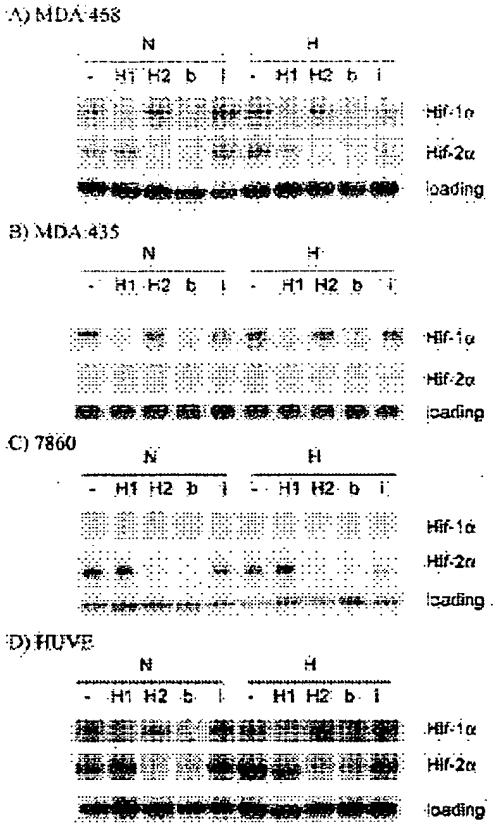

Fig. 1. RNase protection analysis of RNA extracted from MDA 468 cells (*A*), MDA 435 cells (*B*), 786-0 cells (*C*), and HUVECs (*D*). Cells were mock transfected (−) or subjected to siRNA directed to Hif-1α (1), Hif-2α (2), both Hif-1α and Hif-2α (b), or inverted control (i) before subsequent incubation for 16 h in 20% oxygen (N) or 0.1% oxygen (H). Specific down-regulation of Hif-1α or Hif-2α mRNA occurred after siRNA for each respective transcript or both transcripts. The inverted siRNA control had no effect on mRNA levels. Quantification of U6 small nuclear RNA was used as a loading control.

Hif-2α mRNAs were synthesized and transfected into MDA 468 cells, which were then subjected to hypoxic stimulation. The results obtained with these siRNAs were the same as described above in respect to specificity of Hif-1α and Hif-2α targeting (data not shown).

Expression of Hypoxically Induced Genes by Human Cell Lines After Treatment with siRNA for Hif-1α and Hif-2α. The HIF system up-regulates the production of proteins with a wide range of functions in the homeostatic and apoptotic response (2, 3, 13, 15) to hypoxia and cell death in many different human cell types. To investigate the importance of Hif-1α and Hif-2α in conferring such responses in different cell backgrounds, we analyzed the expression of CA9 (acid metabolism), BNip3 (cell death), GLUT-1 (glucose/energy metabolism), VEGF (angiogenesis), and uPAR (proteolytic pathway of invasion) in MDA 435 cells, MDA 468 cells (breast carcinoma), 786-0 cells (renal carcinoma), and HUVECs (endothelial) after treatment with Hif-1α and/or Hif-2α siRNA. Protein levels were measured using Western blot analysis (CA9, BNip3, and GLUT-1) or ELISA (VEGF and uPAR).

Analysis of the breast carcinoma cell lines revealed that MDA 468 cells expressed both Hif-1α and Hif-2α protein (Fig. 2), whereas MDA 435 cells expressed only Hif-1α protein (data not shown). In both cell lines, hypoxic induction of CA9, BNip3, GLUT-1, VEGF, and uPAR protein was inhibited by treatment with Hif-1α siRNA but not affected by Hif-2α siRNA. Silencing both Hif-1α and Hif-2α had the same effect as silencing with Hif-1α, and the inverted control

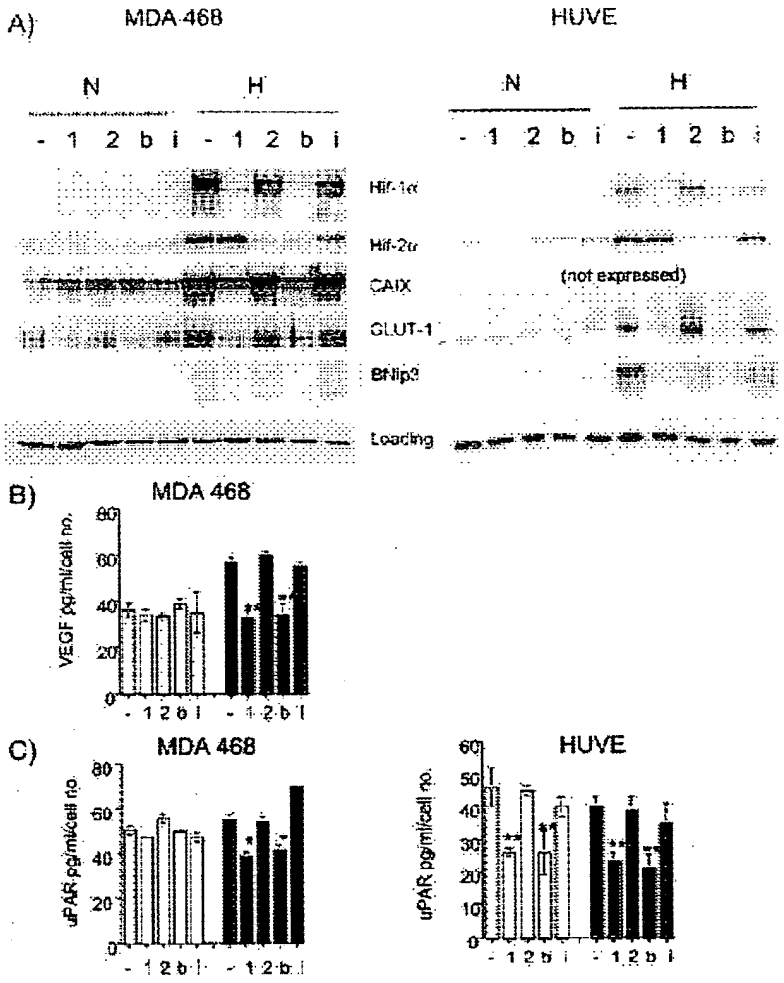

Fig. 2. *A*, Western blot analysis of protein extracted from MDA 468 cells and HUVECs after treatment as described in Fig. 1. Specific down-regulation of Hif-1α or Hif-2α protein occurred after siRNA for each respective transcript or both transcripts. The inverted siRNA control had no effect on protein levels. Hypoxic induction of CA9, GLUT-1, and BNip3 protein was blocked after siRNA for Hif-1α but not after siRNA for Hif-2α. siRNA against both genes also resulted in the down-regulation of the target genes. *B*, VEGF levels and uPAR levels (*C*) in media conditioned by MDA 468 (*B* and *C*) and HUVECs (*C*), normalized to final cell number. Normoxic or hypoxic treatment of cells is indicated by □ and ■, respectively. Experiments were performed in triplicate at least three times, and results from one representative experiment are shown. One-tailed, student *t* tests comparing each treatment with the hypoxic mock control were performed, and significance is indicated by * for $P < 0.05$ and ** for $P < 0.01$.

siRNA had no effect on the expression of any of the genes (Fig. 2; data not shown). The same results were obtained when MDA 468 cells were transfected with the confirmatory siRNAs (data not shown).

Similar to the MDA 468 cell lines, HUVECs expressed both Hif-1α and Hif-2α protein after hypoxic stimulus (Fig. 2). Hypoxia did not induce HUVECs to express CA9 or secrete VEGF but did increase the levels of expression of BNip3, GLUT-1, and uPAR. Pretreatment of HUVECs with siRNA to Hif-1α ablated the hypoxic induction of BNip3, GLUT-1, and uPAR, but Hif-2α siRNA treatment had no effect on protein production (Fig. 2).

The renal carcinoma cell line 786-0 expressed Hif-2α but not Hif-1α, and because this cell line lacks functional VHL, expression of Hif-2α was seen constitutively under normoxic conditions (Fig. 3). VEGF and GLUT-1 proteins were also constitutively expressed, but BNip3 and CA9 proteins were not expressed at detectable levels. uPAR was constitutively expressed by 786-0 cells but at 2-fold lower levels than by breast or endothelial cells. Treatment of cells with siRNA to Hif-2α reduced the expression of GLUT-1 and VEGF, whereas siRNA to Hif-1α had no effect (Fig. 3). Expression of uPAR was not affected by siRNA to Hif-1α or Hif-2α.

Cell Migration Induced by Hypoxia Is Affected by Pretreatment with siRNA to Hif-1α or Hif-2α Depending on the Cell Type. Intratumoral hypoxia is correlated with increased risk of invasion in human cancer (1), and hypoxia increases the invasion of colon carcinoma cells (16). To elucidate which hypoxia-induced transcription factor is involved in this process, we analyzed MDA 468 and HUVE cells treated with siRNA for Hif-1α or Hif-2α and normoxia or hypoxia in a cell migration assay. Cells subjected to hypoxia showed increased migration compared with the cells that had remained in normoxia, and treatment with inverted siRNA or mock transfection had no effect on the migration response. In MDA 435 cells, the hypoxic response was inhibited by treatment with siRNA directed to Hif-1α but not to Hif-2α. However, in MDA 468 and HUVECs, hypoxically induced migration was inhibited by pretreatment of the cells with either Hif-1α or Hif-2α siRNA. Treatment of cells with both siRNAs inhibited the hypoxically induced migration response in both cell lines but not more than with either alone (Fig. 4).

Discussion

In this study, we used siRNAs that specifically target degradation of mRNAs encoding Hif-1 α or Hif-2α. After treatment with siRNA, the expression of Hif-1α or Hif-2α mRNA and protein was greatly reduced under hypoxic conditions. The effects of these siRNAs were analyzed in two human breast carcinoma cell lines, a human endothelial cell line, and a human renal carcinoma cell line containing an inactivating mutation in VHL.

Our results indicate that in the breast carcinoma and endothelial cell

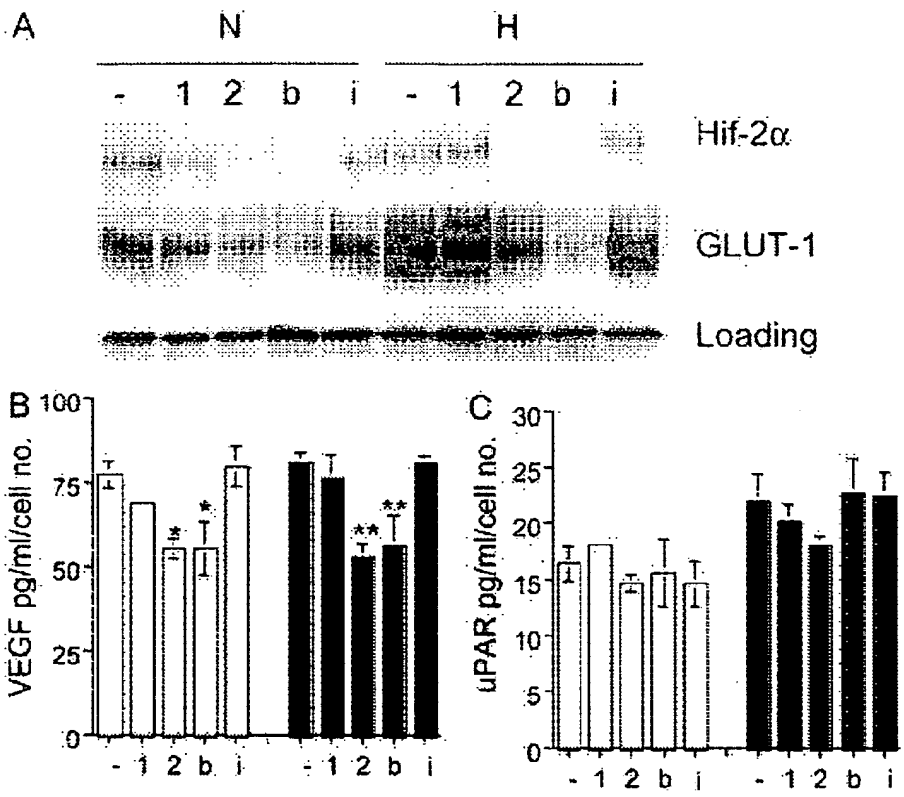

Fig. 3. *A*, Western blot analysis of protein extracted from 786-0 cells after treatment as described in Fig. 1. 786-0 cells do not express Hif-1α, but specific down-regulation of Hif-2α protein occurred after siRNA for Hif-2α. The inverted siRNA and Hif-1α siRNA had no effect on Hif-2α protein levels. GLUT-1 protein is reduced after siRNA for Hif-2α but not after siRNA for Hif-1α. Somewhat unusually, there was a modest induction of GLUT-1 after hypoxic stimulus, which was also inhibited by siRNA for Hif-2α. siRNA for both genes also resulted in the down-regulation of the target genes. *B*, VEGF levels and uPAR levels (*C*) in media conditioned by the above cells normalized to final cell number. Normoxic or hypoxic treatment of cells is indicated by □ and ■, respectively. Experiments were performed in triplicate at least three times, and results from one representative experiment are shown. One-tailed, student *t* tests comparing each treatment with the hypoxic mock control were performed, and significance is indicated by * for $P < 0.05$ and ** for $P < 0.01$.

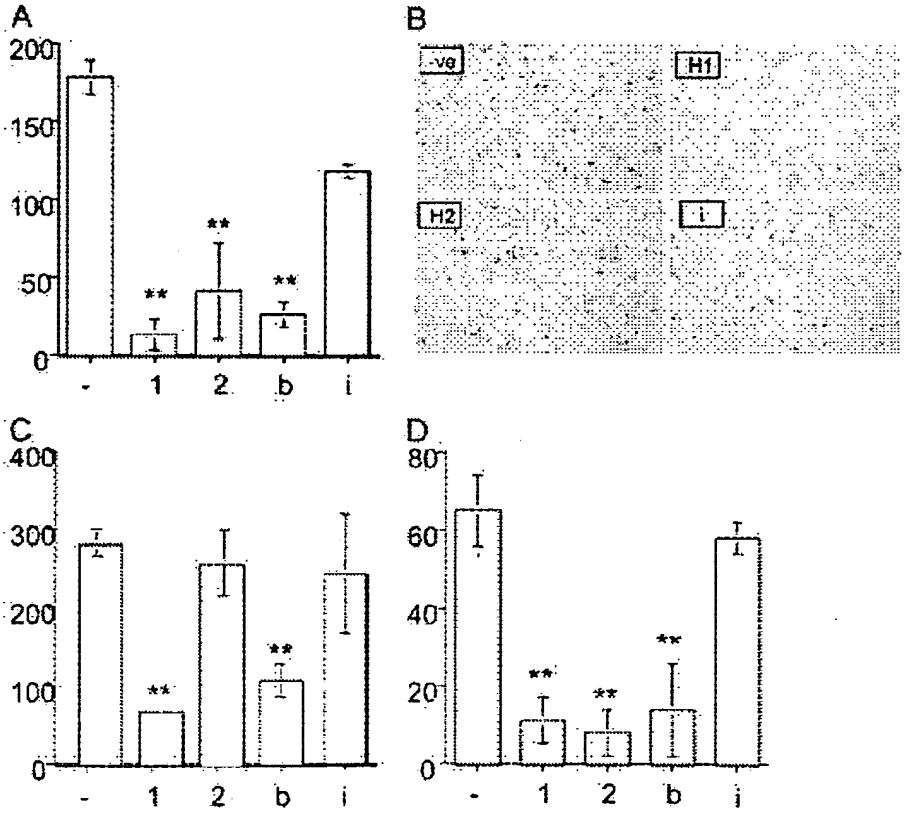

Fig. 4. Migration analysis of cells treated with a mock transfection (−) or siRNA for Hif-1α (1), Hif-2α (2), both Hif-1α and Hif-2α (b), or inverted control (i) before subsequent incubation for 16 h in 0.1% oxygen. The number of cells that had migrated through an 8-μm filter was counted, and the mean and SD of three replicates in a representative experiment is shown graphically. *A* and *B*, hypoxically induced migration of MDA 468 cells is inhibited by treatment with siRNA for both Hif-1α and Hif-2α. *B* shows photographs of the bottom of a representative selection of migration chambers, with blue cells visible around the smaller round pores of the filter. *C*, hypoxically induced migration of MDA 435 cells was inhibited by treatment with siRNA for Hif-1α, not Hif-2α, whereas migration of HUVECs was inhibited by siRNA for both Hif-1α and Hif-2α (*D*).

lines, the major Hif-α isoform required for induction of a set of well-characterized hypoxic genes is Hif-1α. Surprisingly, even in cells expressing both Hif-α isoforms, Hif-2α did not substitute in regulating any of these genes when Hif-1α was inactivated. Nevertheless, functional analysis of the endothelial and breast carcinoma cell lines revealed that both Hif-1α and Hif-2α are required for hypoxia-induced cell migration in cell lines that express both proteins, suggesting that there are other actions of Hif-2α that have not been revealed in our studies of gene expression. Overall, however, the importance of Hif-1α in these cells is in concordance with other studies that have reported Hif-1α as a positive factor in tumor growth (17) and carcinoma cell invasion (16) in different cells. The hypothesis that Hif-1α is the major hypoxia-induced transcription factor involved in breast carcinogenesis is supported by evidence that one of the breast carcinoma cell lines used in this study has lost Hif-2α expression, and stable transfection of this cell line with Hif-2α resulted in its impaired growth as xenograft tumors compared with the parental line (10).

In contrast with the above results, we found that in the VHL-defective 786-0 renal carcinoma line, in which the native Hif-1α gene is not expressed, some of the hypoxia-inducible transcripts were now critically dependent of Hif-2α. VHL is required for proteolytic regulation of both Hif-1α and Hif-2α, and in VHL defective cells both isoforms are stabilized. However, there is an unusual bias toward enhanced Hif-2α mRNA expression in clear cell renal carcinoma that is not observed in the renal tubular epithelium from which these tumors are derived (7) but arises during tumor development (18). This may be because of an additional action of VHL on the Hif system (19, 20) and/or additional non-VHL mediated actions on Hifα isoforms that arise during the oncogenic process. The current results suggest the existence of another distinct interface between the HIF system and renal carcinogenesis that makes connections between Hif-2α expression and certain hypoxia-inducible mRNAs. The finding that the Hif-2α pathway appears to be specifically activated in clear cell renal carcinogenesis by several steps strongly suggests a causal role for Hif-2α in development of the cancer. Interestingly, this is supported by comparison of results from two groups that have examined the expression of mutant forms of Hif-1α or Hif-2α that escape VHL-mediated destruction on the tumor suppressor effect of expressing wild-type VHL in renal cell carcinoma cells. These studies have shown that stabilized Hif-2α but not Hif-1α reverses VHL tumor suppressor function (8, 9).

In conclusion, these studies have, for the first time, directly compared functional inactivation of Hif-1α and Hif-2α in different cancer cell lines. The findings indicate that the actions are distinct and differ according to cell background and suggest that these differences are important in tumor development.

Acknowledgments

We thank Arnold Greenberg (deceased) of the cell death group at Manitoba Institute of Cell Biology, University of Manitoba (Winnipeg, Manitoba, Canada) for the kind gift of the BNip3 monoclonal antibody.

References

1. Hoeckel, M., and Vaupel, P. Biological consequences of tumor hypoxia. Semin. Oncol., *28:* 36–41, 2001.
2. Semenza, G. L. HIF-1 and tumor progression: pathophysiology and therapeutics. Trends Mol. Med., *8:* S62–S67, 2002.
3. Pugh, C. W., and Ratcliffe, P. J. Regulation of angiogenesis by hypoxia: role of the HIF system. Nat. Med., *9:* 677–684, 2003.
4. Wiesener, M. S., Turley, H., Allen, W. E., Willam, C., Eckhardt, K. U., Talks, K. L., Wood, S. M., Gatter, K. C., Harris, A. L., Pugh, C. W., Ratcliffe, P. J., and Maxwell, P. H. Induction of endothelial PAS domain protein-1 by hypoxia: characterization and comparison with hypoxia-inducible factor-1α. Blood, *92:* 2260–2268, 1998.
5. Ema, M., Hirota, K., Mimura, J., Abe, H., Yodoi, J., Sogawa, K., Poellinger, L., and Fujii-Kuriyama, Y. Molecular mechanisms of transcription activation by HLF and HIF1α in response to hypoxia: their stabilization and redox signal-induced interaction with CBP/p300. EMBO J., *18:* 1905–1914, 1999.
6. Brusselmans, K., Bono, F., Maxwell, P. H., Dor, Y., Dewerchin, M., Collen, D., Herbert, J-M., and Carmeliet, P. Hypoxia-inducible factor-2α is involved in the apoptotic response to hypoglycemia but not to hypoxia. J. Biol. Chem., *276:* 39192–39196, 2001.
7. Rosenberger, C., Mandriota, S., Jurgensen, J. S., Wiesner, M. S., Horstrup, J. H., Frei, U., Ratcliffe, P. J., Maxwell, P. H., Bachmann, S., and Eckardt, K. U. Expression of hypoxia-inducible factor-1α and -2α in hypoxic and ischemic rat kidneys. J. Am. Soc. Nephrol., *13:* 1974–1976, 2002.
8. Maranchie, J. K., Vasselli, J. R., Riss, J., Bonifacino, J. S., Linehan, W. M., and Klausner, R. D. The contribution of VHL substrate binding and HIF-1α to the phenotype of VHL loss in renal cell carcinoma. Cancer Cell, *1:* 247–255, 2002.
9. Kondo, K., Kleo, J., Nakamura, E., Lechpammer, M., and Kaelin, W. G. Inhibition of HIF is necessary for tumor suppression by the von Hippel Lindau protein. Cancer Cell, *1:* 237–246, 2002.
10. Blancher, C., Moore, J. W., Talks, K. L., Houlbrook, S., and Harris, A. L. Relationship of hypoxia-inducible factor (HIF)-1α and HIF-2α expression to vascular endothelial growth factor induction and hypoxia survival in human breast cancer cell lines. Cancer Res., *60:* 7106–7113, 2000.
11. Elbashir, S. M., Harborth, J., Lendeckel, W., Yalcin, A., Weber, K., and Tuschl, T. Duplexes of 21-nucleotide RNAs mediate RNA interference in cultured mammalian cells. Nature (Lond.), *411:* 494–498, 2001.
12. Chomczynski, P., and Sacchi, N. Single step method of RNA isolation by acid guanidinium thiocyanate-phenol-chloroform extraction. Anal. Biochem., *162:* 156–159, 1987.
13. Wykoff, C. C., Beasley, N. J. P., Watson, P. H., Turner, K. J., Pastorek, J., Sibtain, A., Wilson, G. D., Turley, H., Talks, K., Maxwell, P. H., Pugh, C. W., Ratcliffe, P. J., and Harris, A. L. Hypoxia-inducible expression of tumor-associated carbonic anhydrases. Cancer Res., *60:* 7075–7083, 2000.
14. Ray, R., Chen, G., Vande Velde, C., Cizeau, J., Hoon Park, J. H., Reed, J. C., Gietz, R. D., and Greenberg, A. H. BNIP3 heterodimerizes with Bcl-2/Bcl-XL and induces cell death independent of a Bcl-2 homology 3 (BH3) domain at both mitochondrial and nonmitochondrial sites. J. Biol. Chem., *275:* 1439–1448, 2000.
15. Sowter, H. M., Ratcliffe, P. J., Watson, P., Greenberg, A. H., and Harris, A. L. HIF-1-dependent regulation of hypoxic induction of the cell death factors BNIP3 and NIX in human tumors. Cancer Res. *61:* 6669–6673, 2001.
16. Kristnamachary, B., Berg-Dixon, S., Kelly, B., Agani, F., Feldser, D., Ferreira, G., Iyer, N., LaRusch, J., Pak, B., Taghavi, P., and G. L. S. Regulation of colon carcinoma cell invasion by hypoxia-inducible factor 1. Cancer Res., *63:* 1138–1143, 2003.
17. Ryan, H. E., Poloni, M., McNulty, W., Elson, D., Gassmann, M., Arbeit, J. M., and Johnson, R. S. Hypoxia-inducible factor-1α is a positive factor in solid tumor growth. Cancer Res., *60:* 4010–4015, 2000.
18. Mandriota, S. J., Turner, K. J., Davies, D. R., Murray, P. G., Morgan, N. V., Sowter, H. M., Wykoff, C. C., Maher, E. R., Harris, A. L., Ratcliffe, P. J., and Maxwell, P. H. HIF inactivation identifies early lesions in VHL kidneys: evidence for site specific tumor suppressor function in the nephron. Cancer Cell, *1:* 459–468, 2002.
19. Kreig, M., Haas, R., Brauch, H., Acker, T., Flamme, I., and Plate, K. H. Up-regulation of hypoxia-inducible factors HIF-1α and HIF-2α under normoxic conditions in renal carcinoma cells by von Hippel-Lindau tumor suppressor gene loss function. Oncogene, *19:* 5435–5443, 2000.
20. Maxwell, P. H., Dachs, G., Gleadle, J. M., Nicholls, L. G., Harris, A. L., Stratford, I. J., Hankinson, O., Pugh, C. W., and Ratcliffe, P. J. Hypoxia-inducible factor-1 modulates gene expression in solid tumors and influences both angiogenesis and tumor growth. Proc. Natl. Acad. Sci. USA, *94:* 8104–8109, 1997.

Structural basis for PAS domain heterodimerization in the basic helix–loop–helix-PAS transcription factor hypoxia-inducible factor

Paul J. A. Erbel*†, Paul B. Card*†, Ozgur Karakuzu*, Richard K. Bruick*, and Kevin H. Gardner*†‡

Departments of *Biochemistry and †Pharmacology, University of Texas Southwestern Medical Center, 5323 Harry Hines Boulevard, Dallas, TX 75390

Edited by Susan S. Taylor, University of California at San Diego, La Jolla, CA, and approved October 9, 2003 (received for review June 10, 2003)

Biological responses to oxygen availability play important roles in development, physiological homeostasis, and many disease processes. In mammalian cells, this adaptation is mediated in part by a conserved pathway centered on the hypoxia-inducible factor (HIF). HIF is a heterodimeric protein complex composed of two members of the basic helix–loop–helix Per-ARNT-Sim (PAS) (ARNT, aryl hydrocarbon receptor nuclear translocator) domain family of transcriptional activators, HIFα and ARNT. Although this complex involves protein–protein interactions mediated by basic helix–loop–helix and PAS domains in both proteins, the role played by the PAS domains is poorly understood. To address this issue, we have studied the structure and interactions of the C-terminal PAS domain of human HIF-2α by NMR spectroscopy. We demonstrate that HIF-2α PAS-B binds the analogous ARNT domain *in vitro*, showing that residues involved in this interaction are located on the solvent-exposed side of the HIF-2α central β-sheet. Mutating residues at this surface not only disrupts the interaction between isolated PAS domains *in vitro* but also interferes with the ability of full-length HIF to respond to hypoxia in living cells. Extending our findings to other PAS domains, we find that this β-sheet interface is widely used for both intra- and intermolecular interactions, suggesting a basis of specificity and regulation of many types of PAS-containing signaling proteins.

Cellular responses to oxygen availability are essential for the development and homeostasis of mammalian cells, demonstrated most critically by the link between the cellular adaptation to reduced tissue oxygenation and disease progression (1, 2). In mammalian cells, these responses are mediated in part by the hypoxia-inducible factor (HIF), a heterodimeric transcription factor composed of HIFα and aryl hydrocarbon receptor nuclear translocator (ARNT, also known as HIFβ) (3). HIF activity is tightly controlled under normoxic conditions by multiple O_2-dependent hydroxylation events of the HIFα subunit, which coordinately promote the ubiquitin-mediated destruction of this protein (4) and impair its ability to interact with transcriptional coactivators (5, 6) (Fig. 1*a*). These controls are relieved during hypoxia, allowing HIF to activate the transcription of genes that facilitate metabolic adaptation to low oxygen levels and increase local oxygen supply by angiogenesis (7).

All three isoforms of HIFα [HIF-1α, -2α (EPAS1), and -3α] (8, 9) and ARNT belong to the basic helix–loop–helix (bHLH)–Per-ARNT-Sim (PAS) family of eukaryotic transcription factors, which contain bHLH and PAS domains (Fig. 1). The bHLH domains of these proteins serve as dimerization elements, helping determine the specificity of complex formation while providing a DNA-binding interface composed of the basic regions from each monomer (10). PAS domains are widespread components of signal transduction proteins, currently identified in >2,000 proteins from organisms in all three kingdoms of life. These domains, shown to be protein–protein interaction elements in several systems (11), also appear to contribute to the dimerization process and thus increase the specificity of bHLH-PAS transcription factor formation (12, 13). In the case of the HIFα/ARNT complex, coimmunoprecipitation and gel mobility-shift experiments using truncated forms of HIFα and ARNT suggest that although the bHLH domains alone are able to dimerize, the PAS domains are required to build a stable heterodimer capable of robust DNA binding (14, 15). These data suggest a model of the complex where the bHLH, PAS-A, and PAS-B domains of ARNT interact with their counterparts in HIFα (Fig. 1*a*). However, most of this model remains speculative in light of the sparse data describing how PAS domains bind to each other, or more generally, to any protein partner.

To provide insight into this general topic of PAS domain signaling, particularly its importance in the hypoxia response pathway, we have studied the structure and interactions of the C-terminal PAS domain of human HIF-2α (HIF-2α PAS-B) by NMR spectroscopy. We report that HIF-2α PAS-B adopts a structure similar to other members of this family, with a central β-sheet flanked on one face by several α-helices. We further show that HIF-2α PAS-B binds directly to the human ARNT PAS-B domain *in vitro*, identifying the interface as a group of residues located in the central strands of the β-sheet. With structure-based mutations of this interface in the PAS-B domains of HIF-1α and -2α, we demonstrate that such changes interfere with the binding of isolated PAS-B domains *in vitro* but more importantly disrupt the ability of full-length HIF proteins to respond to hypoxia in living cells. These observations led us to compare PAS domains from multiple systems, showing that the β-sheet interface participates in a wide range of inter- and intramolecular interactions and suggesting a way that specificity and regulation may be achieved among these versatile domains.

Materials and Methods

Protein Expression and Purification. DNA-encoding fragments of human HIF-2α PAS-B (residues 240–350) and ARNT PAS-B (residues 356–470) were subcloned into the pGβ1-parallel and pHis-parallel expression vectors, respectively (16, 17). *Escherichia coli* BL21(DE3) cells transformed with these plasmids were grown in M9 media containing 1 g/liter $^{15}NH_4Cl$ for U-^{15}N samples (supplemented with 3 g/liter $^{13}C_6$ glucose for U-$^{15}N/^{13}C$ labeled samples). These cultures were grown at 37°C to an A_{600} of 0.6–1.0, then induced overnight at 20°C by the addition of 0.5 mM isopropyl β-D-thiogalactoside.

The purification of HIF-2α PAS-B has been detailed (18). NMR samples typically contained 0.9 mM protein in 50 mM Tris buffer (pH 7.3), 15 mM NaCl, 5 mM DTT, 5 mM NaN_3 and a protease inhibitor mixture (Sigma) in 90% H_2O/10% D_2O,

This paper was submitted directly (Track II) to the PNAS office

Abbreviations: HIF, hypoxia-inducible factor; PAS, Per-ARNT-Sim; HIF-2α PAS-B, C-terminal PAS domain of human HIF-2α; ARNT, aryl hydrocarbon receptor nuclear translocator; bHLH, basic helix–loop–helix; HSQC, heteronuclear sequential quantum correlation; CHO, Chinese hamster ovary; HRE, hypoxia responsive element.

Data deposition: The atomic coordinates for the HIF-2α PAS-B domain have been deposited in the Protein Data Bank (PDB ID 1P97).

‡To whom correspondence should be addressed. E-mail: kevin.gardner@utsouthwestern.edu.

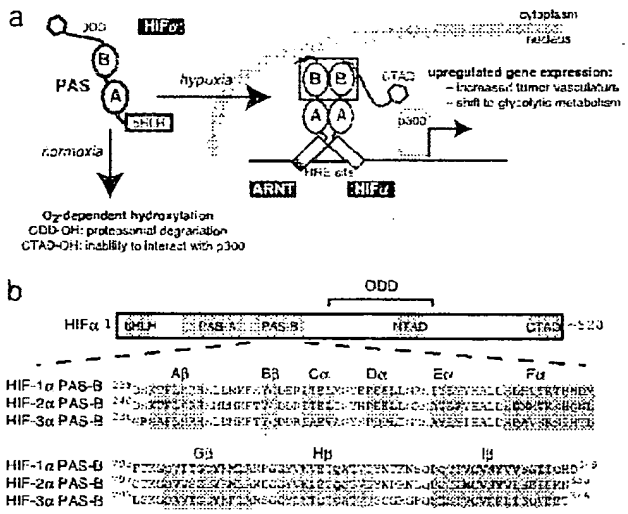

Fig. 1. Oxygen-dependent regulation and domain architecture of HIF proteins. (*a*) HIF regulation is tightly linked to intracellular oxygen levels. Under normoxic conditions, HIFα is posttranslationally hydroxylated, promoting its degradation (modification of the oxygen-dependent degradation domain (ODD)) and interfering with its ability to interact with CBP/p300 coactivators (modification of the transcriptional activation domains NTAD and CTAD). These modifications are not made under hypoxic conditions, allowing HIFα to accumulate and enter the nucleus where it associates with ARNT and binds to HREs upstream of hypoxia-activated genes. The red box highlights the HIFα and ARNT PAS-B domains. (*b*) Domain topology of HIFα subunits, including a bHLH domain, two PAS domains, and C-terminal regulatory domains. A sequence alignment of the HIFα PAS-B orthologs is shown, with bold letters indicating the mutated residues described in the text. HIF-2α PAS-B secondary structure elements are indicated with a gray background.

unless otherwise noted. ARNT PAS-B was expressed and purified as described in *Supporting Methods*, which is published as supporting information on the PNAS web site.

Parallel studies on human HIF-1α PAS-B used a construct containing residues 238–349, chosen by homology with HIF-2α PAS-B. Expression and purification of HIF-1α PAS-B were done as described for HIF-2α PAS-B.

NMR Spectroscopy. All NMR data were recorded at 30°C with Varian Inova 500 and 600 MHz spectrometers by using NMRPIPE for data processing (19) and NMRVIEW for analysis (20). Chemical-shift assignments were made by using standard methods (21) as detailed in *Supporting Methods*.

Deuterium exchange reactions were started by resuspending lyophilized ^{15}N-labeled HIF-2α PAS-B in 99% D_2O (uncorrected pH 7.3). These samples were then placed into a prewarmed magnet (T = 30°C), and ^{15}N/^{1}H heteronuclear sequential quantum correlation (HSQC) spectra were sequentially acquired approximately every 15 min. Observed ^{1}H exchange rates were converted into protection factors by using standard methods (22).

Structure Determination. Interproton distance constraints were obtained from 3D ^{15}N edited NOESY (τ_m = 150 ms), ^{15}N, ^{13}C edited NOESY (τ_m = 100 ms), and 2D NOESY (τ_m = 120 ms) spectra. Hydrogen bond constraints (1.3 Å < d_{NH-O} < 2.5 Å, 2.3 Å < d_{N-O} < 3.5 Å) were set for backbone amide protons protected for >30 min from exchange with D_2O solvent (30°C, pH 7.3). Constraints for the ϕ and ψ dihedral angles were generated by chemical-shift analyses by using TALOS (23), with two times the standard deviation of TALOS predictions as the bounds (minimum ± 30°). For 19 residues without TALOS predictions, ϕ dihedral angle constraints were obtained from an analysis of a 3D HNHA spectrum. Finally, 78 ^{15}N-^{1}H residual dipolar coupling constraints were obtained from a sample partially aligned in 5% (wt/vol) DMPC/DHPC ratio of 3:1 (Avanti Polar Lipids) and 5 mM cetyltrimethylammonium bromide at 35°C.

Initial structures were determined without manual assignments by using ARIA1.2 (24, 25) and subsequently refined with a mix of automated and manual assignment of NOESY spectra. Of 1,000 structures, the 20 lowest-energy structures were analyzed with MOLMOL (26) and PROCHECK-NMR (27).

From this ensemble, the structure closest to the mean was superimposed against other PAS domains with the DEEPVIEW Swiss Protein Data Bank program (28) with the automatic fit option. The calculated rms deviations ranged between 1.4 and 1.65 Å for HERG (Research Collaboratory for Structural Bioinformatics Protein Data Bank ID 1BYW), hPASK (1LL8), RmFixL (1D06), and Phy3 (1G28). The HIF-2α PAS-B structure was also used to generate a model of the HIF-1α PAS-B structure (74% sequence identity) by using MODELLER (29).

HIFα and ARNT PAS-B Titration. Titrations were conducted by the stepwise addition of natural abundance ARNT PAS-B (up to 800 μM) to a sample of 200-μM HIF-2α at 35°C. The peak heights of HIF-2α PAS-B signals that do not show ARNT-dependent chemical shift changes (38 residues) were fit to Eq. 1 to obtain the corresponding K_d:

$$\Delta I = 1 - \{\Delta I_{max} \times [(A + P_T + K_d) - ((A + P_T + K_d)^2 - (4 \times A \times P_T))^{1/2}]/[2 \times P_T]\}, \quad [1]$$

where ΔI is the observed change in peak height at ARNT concentration A, ΔI_{max} is the change in peak height at saturation, and P_T is the total HIFα concentration. Eq. 1 is similar to the equation used to extract K_d from chemical-shift changes observed in titrations of complexes undergoing fast exchange (30), and we apply it here only to sites without chemical-shift changes (fast exchange) to ensure that the observed peak line widths are a population-weighted average of the free- and bound-state line widths (31). The binding of HIF-2α PAS-B mutants to ARNT PAS-B was assessed by adding 900 μM natural abundant ARNT PAS-B to 250 μM HIFα PAS B at 25°C.

Mutagenesis. Point mutants of full-length HIF-1α and -2α were created from wild-type DNA and primers including the desired mutation(s). PAS-B domains containing these mutations were obtained by PCR amplification of the corresponding full-length sequence and subcloned into the pGβ1-parallel vector. Transformation, protein induction, and purification were performed as described above.

Transfections. Cells were plated onto 48-well plates (3.5×10^4 cells per well) in 200 μl of HyQ DME/F-12 1:1 media (HyClone) supplemented with 5% FBS 24 h before transfection. Cells were transfected with 10 ng of each HIFα construct and 20 ng of the 3HRE-tk-luc (HRE, hypoxia-responsive element) luciferase reporter construct (8) by using the Lipofectamine PLUS reagent (Invitrogen). After 3 h, the media were changed and, after an additional 2 h, cells were incubated for 15 h under normoxic or hypoxic (1.0% O_2) conditions. Luciferase activity was measured as described (32).

Results

Solution Structure of HIF-2α PAS-B. We determined the solution structure of HIF-2α PAS-B by using standard double- and triple-resonance NMR experiments conducted on uniformly ^{15}N and ^{15}N ^{13}C labeled protein samples (Fig. 2). This structure is

BIOPHYSICS

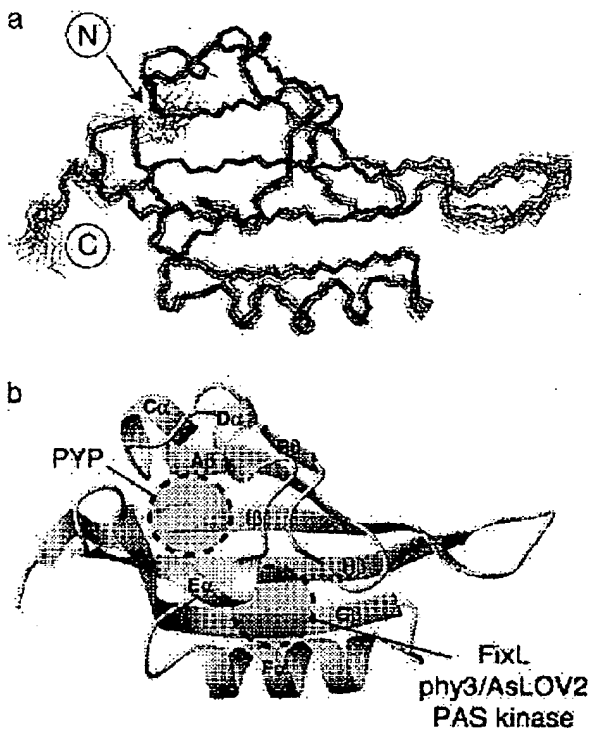

Fig. 2. Solution structure of HIF-2α PAS-B. (*a*) Superimposition of 20 lowest-energy structures for HIF-2α PAS-B, calculated as indicated in the text. (*b*) Ribbon diagram of the structure closest to the mean of the ensemble shown in *a*. Circles indicate the approximate locations of the ligand-binding sites of several PAS domains (17, 33–36).

Table 1. Statistics for HIF-2α PAS-B solution structure determination

List of constraints	
NOE distance restraints	
Unambiguous	2,767
Ambiguous	496
Hydrogen bond restraints	60
Dihedral angle restraints	96
^{15}N-^{1}H residual dipolar couplings	78
Stereospecific assignments (Val γ, Leu δ)	12
Structural analysis	
Mean rms deviation from experimental restraints	
NOE, Å	0.022 +/− 0.002
Dihedral angles, deg	1.04 +/− 0.16
Average number of:	
NOE violations >0.5 Å	0
NOE violations >0.3 Å	1.9 +/− 1.2
Dihedral violations >5°	1.6 +/− 1.1
Mean rms from idealized covalent geometry	
Bonds, Å	0.0045
Angles, deg.	0.65
Impropers, deg.	1.69
Geometric analysis of residues 6–91 and 98–112	
rms deviation to mean	0.53 +/− 0.07 Å (backbone) 1.08 +/− 0.10 Å (all heavy)
Ramachandran analysis (PROCHECK)	81.0% most-favored 16.4% additionally allowed 1.6% generously allowed 1.0% disfavored

based on >2,500 geometric constraints obtained from measurements of interproton distances, dihedral angles, and ^{15}N-^{1}H residual dipolar couplings of a partially oriented sample (Table 1). All of these data are well satisfied by the high-precision ensemble of the 20 lowest-energy structures subsequently used for further analysis.

HIF-2α PAS-B adopts a typical α/β PAS domain fold, characterized by several α-helices flanking a five-stranded antiparallel β sheet. The similarity of this structure to other PAS domains is demonstrated by the low-backbone rms deviation values (1.4–1.65 Å) of pairwise comparisons between representative PAS structures and HIF-2α PAS-B. Although several other PAS domains bind cofactors within their hydrophobic cores to regulate protein–protein interactions in response to various physical stimuli (11), a combination of NMR, mass spectrometry, and visible spectroscopy shows that HIF-2α PAS-B does not copurify with any such compound (data not shown). Further, no preformed cavities are present in the protein core, even at sites occupied by ligands in some other PAS domains (17, 33–36) (Fig. 2*b*).

Identification of ARNT PAS-B-Binding Surface on HIF-2α PAS-B. The PAS domains in bHLH-PAS transcription factors are thought to cooperate with the bHLH domains to facilitate dimerization (12, 13), which implies that the HIFα and ARNT PAS domains bind to each other (Fig. 1*a*). To experimentally demonstrate this interaction, we titrated unlabeled ARNT PAS-B into ^{15}N-labeled HIF-2α PAS-B and monitored changes in the HIF-2α ^{15}N/^{1}H HSQC spectrum (Fig. 3*a*). Peaks in these spectra showed both chemical-shift changes and line broadening on addition of ARNT PAS-B, consistent with binding on the intermediate and fast exchange time scales. In contrast, we found that HIF-2α PAS-B signals were not affected by the addition of a PAS domain from PAS kinase, a protein not involved in the hypoxia response (17) (data not shown), suggesting that the changes observed on addition of ARNT PAS-B reflect a specific HIF-2α/ARNT interaction.

The ARNT-induced changes in the HIF-2α line widths demonstrate two important effects. First, we observed a general increase in line width for HIF-2α peaks during the titration, which we attribute to the slower tumbling of the larger 27-kDa heterodimeric complex compared with an isolated HIF-2α PAS-B domain. By monitoring this broadening via the decrease in peak heights as ARNT PAS-B was added, we observed a titration consistent with a 1:1 binding event with a 30 μM K_d (Fig. 3*b*). This effect saturated at a 1:3 (HIF/ARNT) ratio, establishing that it is not caused by nonspecific increases in sample viscosity or aggregation. Second, we observed that a subset of residues preferentially broadened on the addition of substoichiometric amounts of ARNT PAS-B. Such differential effects have been observed in several complexes (17, 37, 38) and arise from exchange broadening at sites experiencing significant chemical-shift changes on complex formation. Mapping sites that exhibit either this differential broadening or significant ARNT-induced chemical shift changes onto the HIF-2α PAS-B structure shows that they cluster on the face of the central β-sheet (Fig. 4). This provides a chiefly hydrophobic surface for ARNT binding that is conserved among the HIF isoforms (Fig. 1), suggesting that the PAS-B domains of all three interact similarly with ARNT.

Evidence for the importance of this interface in the HIF/ARNT PAS-B dimer was obtained from studies of PAS-B domains containing point mutations. Based on our structure, we altered three

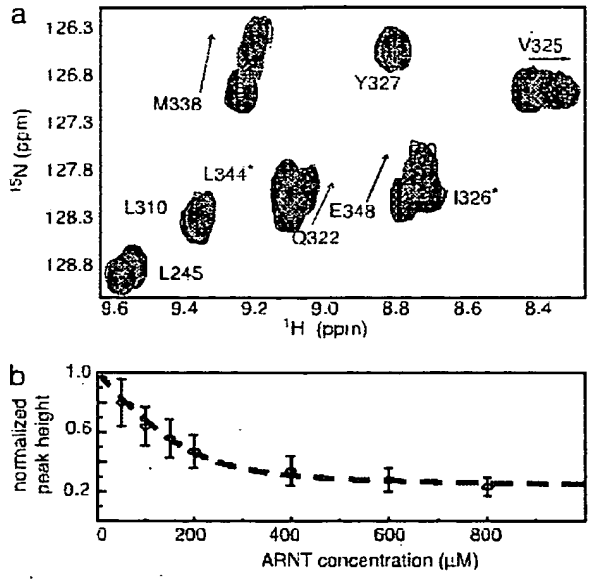

Fig. 3. Characterization of the HIF-2α/ARNT PAS-B-binding interaction. (*a*) Titration of unlabeled ARNT PAS-B (black, 0 μM; light blue, 200 μM; blue, 600 μM; red, 800 μM ARNT) into a 200 μM ^{15}N-labeled HIF-2α PAS-B solution. Arrow shows direction of peak shifts with increasing amounts of ARNT. Residues with peak broadening beyond detection during the titration are indicated with *. (*b*) Normalized peak heights of HIF-2α PAS-B (38 resonances) plotted against increasing amounts of ARNT PAS-B. The concentration dependence of the observed reduction in peak heights can be fit to a 1:1 binding event with a K_d of ~30 μM (dotted line).

residues with solvent-exposed side chains within the Hβ and Iβ strands (Q322E, M338E, and Y342T) (Fig. 4*b*). ^{15}N/^{1}H HSQC spectra of this triple mutant (trHIF-2α PAS-B) retain the chemical-shift dispersion and general pattern of the wild-type protein, confirming that the protein structure remains intact (Fig. 5*a*). The ARNT-binding capability of this mutant was assessed by comparing ^{15}N/^{1}H HSQC spectra before and after addition of unlabeled ARNT PAS-B. As demonstrated by the minimal ARNT-induced changes in peak locations and intensities, the interaction of the triple mutant HIF-2α PAS-B with ARNT has been very significantly weakened. These data establish that subtle changes on the surface of the Hβ and Iβ strands of HIF-2α PAS-B can disrupt the HIF–ARNT PAS-B interaction.

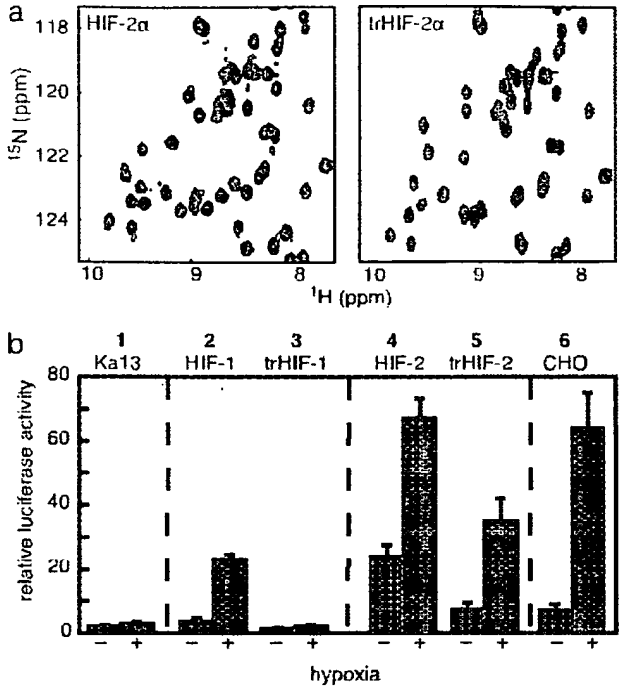

Fig. 5. Point mutations in the HIFα PAS-B central β-sheet disrupt the binding of ARNT PAS-B. (*a*) Superimposed ^{15}N/^{1}H HSQC spectra of 250 μM ^{15}N labeled HIF-2α PAS-B (*Left*) or triple mutant (Q322E/M338E/Y342T) (*Right*). Spectra in the presence of 900 μM unlabeled ARNT PAS-B are shown with red contours; those without ARNT are shown in black contours. Similar data for HIF-1α PAS-B are provided in *Supporting Methods*. (*b*) PAS-B domain interaction is important to form a biologically active HIF/ARNT complex. A construct expressing a luciferase reporter under the control of an HRE promoter was transfected into Ka-13 (columns 1–5) or CHO (column 6) cells along with various HIFα constructs. Values represent the average luciferase activity of three samples, with bars indicating standard error. Luciferase expression was induced by cotransfection of HIF-1α (column 2) or HIF-2α (column 4), particularly under hypoxic conditions. Cotransfection of trHIF-1α (column 3) or trHIF-2α (column 5), full-length HIFα proteins containing the three PAS-B mutations, shows a significant drop in luciferase activity compared with wild-type HIFα.

Comparison of HIF-1α and -2α PAS-B. Sequence alignments of HIF-1α and -2α indicate that the PAS-B domains of these proteins are extremely similar (74% identity; Fig. 1*b*). Nevertheless, the HIF-1α homolog of our HIF-2α PAS-B construct